

Supporting Information

**Redox-Switchable Cycloisomerization of Alkynoic Acids with
Naphthalenediimide-Derived N-Heterocyclic Carbene Complexes**

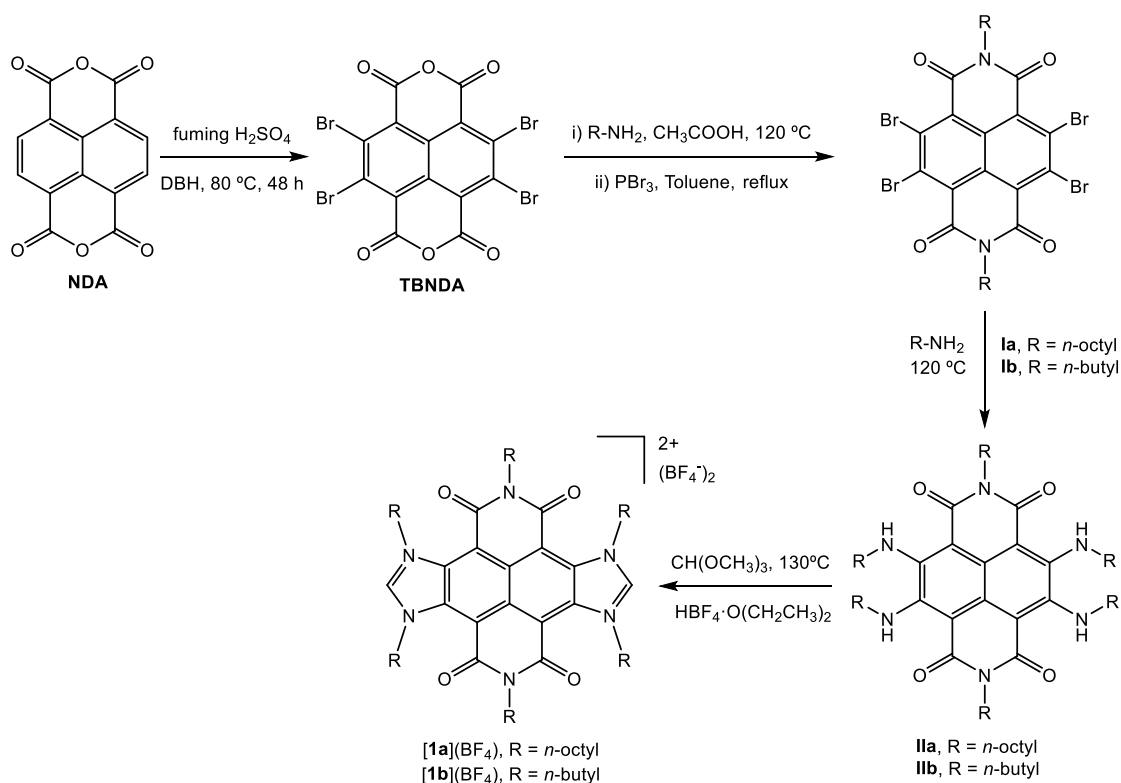
César Ruiz-Zambrana, Ana Gutiérrez-Blanco, Sergio Gonell, Macarena Poyatos, and
Eduardo Peris**

anie_202107973_sm_miscellaneous_information.pdf

| | |
|---|----------------|
| General considerations | S1 |
| 1. Synthesis and characterization of the ligand precursors | S2-S5 |
| 2. Synthesis and characterization of the complexes | S6-S9 |
| 3. Spectroscopic data | S10-S21 |
| 3.1. ¹ H and ¹³ C spectra of 1b in CDCl ₃ | S10 |
| 3.2. ¹ H, ¹³ C and HSQC spectra of [1a](BF ₄) ₂ in CDCl ₃ | S11 |
| 3.3. ¹ H, ¹³ C and HSQC spectra of [1b](BF ₄) ₂ in CD ₃ CN | S12 |
| 3.4. ¹ H, ¹³ C, HSQC and HMBC spectra of 2a in CDCl ₃ | S14 |
| 3.5. ¹ H, ¹³ C and HSQC spectra of 2b in CDCl ₃ | S16 |
| 3.6. ¹ H, ¹³ C and HSQC spectra of 3a in CDCl ₃ | S17 |
| 3.7. ¹ H and ¹³ C spectra of 3b in CDCl ₃ | S19 |
| 3.8. ¹ H and ¹³ C spectra of 4a in CDCl ₃ | S20 |
| 3.9. ¹ H and ¹³ C spectra of 4b in CDCl ₃ | S21 |
| 4. X-Ray crystallography | S22-S24 |
| 5. Electrochemical studies | S25-S29 |
| 5.1 Electrochemical measurements | S25 |
| 5.2 Spectroelectrochemical measurements | S27 |
| 6. Photophysical analysis | S30-S33 |
| 7. Catalytic studies | S33-S35 |
| 8. References | S36 |

General considerations. N,N'-Bis(*n*-octyl)-2,3,6,7-tetrabromonaphthalene diimide (**Ia**) was prepared according to literature methods.^[1] N,N'-Bis(*n*-octyl)-2,3,6,7-tetra(*n*-octylamino)-1,4,5,8-naphthalenecarboxylic diimide (**IIa**)^[2] and N,N'-bis(*n*-butyl)-2,3,6,7-tetra(*n*-butylamino)-1,4,5,8-naphthalenecarboxylic diimide (**IIb**)^[3] were prepared introducing some changes to the reported methods. Anhydrous solvents were dried using a solvent purification system (SPS M BRAUN) or purchased and degassed prior to use by purging them with dry nitrogen. All the other reagents were used as received from the commercial suppliers. NMR spectra were recorded on a Bruker 400 or 300 MHz, using CDCl₃ or CD₃CN as solvents. Signals marked with an asterisk (*) in the NMR spectra correspond to Apiezon brand H grease.^[4] Infrared spectra (FTIR) were performed on a Bruker Equinox 55 spectrometer with a spectral window of 4000-400 cm⁻¹. Electrospray mass spectra (ESI-MS) were recorded on a Micromass Quatro LC instrument; nitrogen was employed as drying and nebulizing gas. UV-Visible absorption spectra were recorded on a Varian Cary 300 BIO spectrophotometer using dry and degassed dichloromethane under ambient conditions. Emission spectra were recorded on a modular Horiba FluoroLog-3 spectrofluorometer employing dry and degassed dichloromethane. Quantum yields were measured using a Hamamatsu integrating sphere at excitation wavelength of 375 nm.

1. Synthesis and characterization of the precursors of the ligands



Scheme S1. Synthesis of the precursors of the ligands

Synthesis of 2,3,6,7-tetrabromonaphthalenetetracarboxylic dianhydride (TBNDA).

In a single-neck round-bottom flask, 1,4,5,8-naphthalenetetracarboxylic dianhydride (NDA) (5 g, 18.6 mmol, 1 equiv.) was suspended in fuming H₂SO₄ (50 mL). The use of fuming H₂SO₄ was found to be crucial for the success of the reaction. The suspension was heated at 55 °C until complete solution of the starting material, which normally takes approximately 2 hours. 5,5-Dimethyl-1,3-dibromohydantoin (DBH) (16 g, 56.0 mmol, 3 equiv.) was then added portion wise, keeping the flask tightly stoppered with a glass stopper between the additions. The resulting suspension was heated at 80 °C in the glass-stoppered round-bottom flask for 48 hours. The resulting brown solution was poured into crushed ice. The obtained solid was isolated by filtration, washed with water and methanol, and dried under vacuum. TBNDA (10.8 g, 99 %) was isolated as a yellow solid. Spectroscopic data were consistent with those reported in the literature.^[2a]

Synthesis of N,N'-bis(*n*-butyl)-2,3,6,7-tetrabromonaphthalene diimide (Ib).

Compound **Ib** was prepared following the reported protocol for N,N'-bis(*n*-octyl)-2,3,6,7-tetrabromonaphthalene diimide (**Ia**).^[1] A suspension of TBNDA (3 g, 5.1 mmol, 1

equiv.) and *n*-butylamine (1.5 mL, 15.3 mmol, 3 equiv.) in acetic acid (50 mL) was stirred at 120 °C. The reaction was stopped when the colour of the reaction mixture changed from yellow to orange, and complete solution of the starting material was observed (45 min approximately). The solvent was then removed under vacuum, and the resulting yellow solid was directly used in the next reaction without further purification. A mixture of the isolated yellow solid and PBr₃ (1.5 mL, 15.8 mmol, 3.1 equiv.) in toluene (100 mL) was refluxed overnight. The solution was allowed to reach room temperature and poured into water (400 mL). The aqueous phase was extracted with toluene (3 x 150 mL), and the combined organic phases were dried over anhydrous MgSO₄. The solvent was removed under reduced pressure and the crude product was washed with methanol and diethyl ether. Compound **Ib** (2.8 g, 80 %) was isolated as an orange solid. ¹H NMR (300 MHz, CDCl₃): δ 4.21 (t, ³J_{H-H} = 8 Hz, 4H, NCH₂CH₂CH₂CH₃), 1.74 (quint, ³J_{H-H} = 8 Hz, 4H, NCH₂CH₂CH₂CH₃), 1.45-1.40 (m, 4H, NCH₂CH₂CH₂CH₃), 1.00 (t, ³J_{H-H} = 8 Hz, 6H, NCH₂CH₂CH₂CH₃). ¹³C{¹H} NMR (75 MHz, CDCl₃): δ 159.93 (C=O), 135.70 (C_q naph), 126.79 (C_q naph), 125.80 (C_q naph), 42.83 (NCH₂CH₂CH₂CH₃), 30.13 (NCH₂CH₂CH₂CH₃), 20.49 (NCH₂CH₂CH₂CH₃), 13.92 (NCH₂CH₂CH₂CH₃).

General procedure for the preparation of diimides **IIa and **IIb**.** In a modification of the procedure reported by Boshale^[2b] and Govindaraju,^[2a] a mixture of **Ia** (or **Ib**) and an excess of *n*-octylamine (or *n*-butylamine) were paced together in a high pressure Schlenk tube fitted with a Teflon cap. The mixture was stirred at 120 °C overnight. After this time, the volatiles were removed under reduced pressure yielding a dark green solid. The crude solid was purified by column chromatography. Elution with a 2:1 hexane/CH₂Cl₂ mixture afforded a green band that contained the desired product.

Synthesis of N,N'-bis-(*n*-octyl)-2,3,6,7-tetra(*n*-octylamino)-1,4,5,8-naphthalenetetracarboxylic diimide (IIa**).** Diimide **IIa** was prepared starting from **Ia** (1 g, 1.2 mmol, 1 equiv.) and *n*-octylamine (2.5 mL, 14.4 mmol, 12 equiv.). After purification by column chromatography, compound **IIa** (555 mg, 45%) was isolated as a dark green solid. Spectroscopic data were consistent with those reported in the literature.^[2]

Synthesis of N,N'-bis-(*n*-butyl)-2,3,6,7-tetra(*n*-butylamino)-1,4,5,8-naphthalenetetracarboxylic diimide (IIb**).** Diimide **IIb** was prepared starting from **Ib** (1 g, 1.4 mmol, 1 equiv.) and *n*-butylamine (3.5 mL, 35 mmol, 25 equiv.). After purification by column chromatography, compound **IIb** (282 mg, 31%) was isolated as a

dark green solid. Spectroscopic data were consistent with those reported in the literature.^[3]

General procedure for the preparation of bis-imidazolium salts [1a](BF₄)₂ and [1b](BF₄)₂. A mixture of diimide **IIa** (or **IIb**), HBF₄ (54 % in diethyl ether) and trimethyl orthoformate were placed together in a Schlenk tube fitted with a Teflon cap. The solution was slowly heated to 130 °C under continuous stirring, keeping these conditions overnight. After this time, the solution was allowed to reach temperature. The Schlenk was carefully opened, and an extra amount of HBF₄ was added to the reaction mixture. The resulting mixture was stirred at 130 °C for 24 hours. After cooling at room temperature, diethyl ether was added to the reaction mixture and the precipitated solid was collected by filtration.

Synthesis of [1a](BF₄)₂. Compound [1a](BF₄)₂ was prepared by reacting **IIa** (200 mg, 0.2 mmol, 1 equiv.) and HBF₄ (0.8 mL, 6 mmol, 30 equiv.) in trimethyl orthoformate (3 mL). An extra amount of HBF₄ (0.8 mL, 6 mmol, 30 equiv.) was needed to achieve full conversion. After the general work-up, compound [1a](BF₄)₂ (105 mg, 44%) was isolated as a yellow crystalline solid. ¹H NMR (400 MHz, CDCl₃): δ 9.68 (s, 2H, NCHN), 4.91 (t, ³J_{H-H} = 8 Hz, 8H, CH₂ Im octyl), 4.23 (t, ³J_{H-H} = 8 Hz, 4H, CH₂ naphth octyl), 1.98-1.86 (m, 8H, CH₂ Im octyl), 1.86-1.76 (m, 4H, CH₂ naphth octyl), 1.46-1.21 (m, 60H, CH₂ octyl), 0.95-0.81 (m, 18H, CH₃ octyl). ¹³C{¹H} NMR (100 MHz, CDCl₃): δ 160.94 (C=O), 154.56 (NCHN), 135.17 (C_q naphth), 123.75 (C_q naphth), 115.63 (C_q naphth), 54.34 (CH₂ Im octyl), 42.62 (CH₂ naphth octyl), 31.99 (CH₂ octyl), 31.91 (CH₂ octyl), 29.97 (CH₂ octyl), 29.44 (CH₂ octyl), 29.39 (CH₂ octyl), 29.17 (CH₂ octyl), 28.35 (CH₂ octyl), 27.32 (CH₂ octyl), 26.49 (CH₂ octyl), 22.78 (CH₂ octyl), 14.21 (CH₃ octyl). Electrospray MS (20 V, *m/z*): 510.9 [M – 2(BF₄)]²⁺, 1108.2 [M – (BF₄)]⁺. (Calcd. for [M – 2(BF₄)]²⁺: 511.4, [M – (BF₄)]⁺: 1108.8).

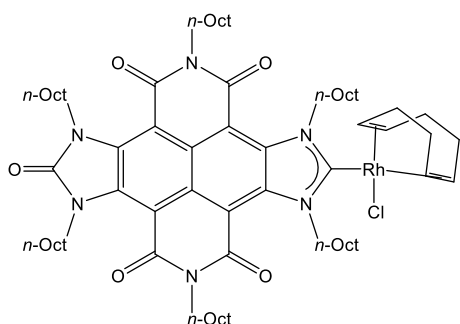
Synthesis of [1b](BF₄)₂. Compound [1b](BF₄)₂ was prepared by reacting **IIb** (200 mg, 0.3 mmol, 1 equiv.) and HBF₄ (1.2 mL, 9 mmol, 30 equiv.) in trimethyl orthoformate (3 mL). An extra amount of HBF₄ (1.2 mL, 9 mmol, 30 equiv.) was needed to achieve full conversion. After the general work-up, compound [1b](BF₄)₂ (183 mg, 71%) was isolated as a yellow crystalline solid. ¹H NMR (300 MHz, CD₃CN): δ 9.62 (s, 2H, NCHN), 4.94 (t, ³J_{H-H} = 8 Hz, 8H, CH₂ Im butyl), 4.25 (t, ³J_{H-H} = 8 Hz, 4H, CH₂ naphth butyl), 1.91-1.76 (m, 12H, CH₂ butyl), 1.59-1.34 (m, 12H, CH₂ butyl), 1.08-0.92 (m, 18H, CH₃ butyl). ¹³C{¹H} NMR (75 MHz, CDCl₃): δ 162.24 (C=O), 155.16 (NCHN), 135.67 (C_q naphth), 124.14 (C_q naphth), 116.65 (C_q naphth), 54.49 (CH₂ Im butyl), 43.00 (CH₂ naphth butyl), 31.97 (CH₂ Im butyl), 30.76

(CH₂ naphth butyl), 20.94 (CH₂ naphth butyl), 20.15 (CH₂ Im butyl), 13.99 (CH₃ naphth butyl), 13.66 (CH₃ Im butyl). Electrospray MS (20 V, *m/z*): 342.5 [M – 2(BF₄)]²⁺, 771.9 [M – (BF₄)]⁺. (Calcd. for [M – 2(BF₄)]²⁺: 342.5, [M – (BF₄)]⁺: 771.7).

2. Synthesis and characterization of metal complexes

General procedure for the preparation of complexes 2a, 2b, 3a and 3b. A mixture of salt [1](BF₄)₂, *t*BuOK and the corresponding metal precursor [MCl(cod)]₂ (M = Rh or Ir) were placed together in a Schlenk flask containing pre-activated molecular sieves (4 Å). Dry and previously deoxygenated THF was added. The resulting mixture was stirred at 40 °C overnight. Once at room temperature, the mixture was filtered through Celite using CH₂Cl₂. The solvent was then removed under reduced pressure. The crude product was purified by column chromatography using CH₂Cl₂ or 1:4 hexane/CH₂Cl₂ as eluent.

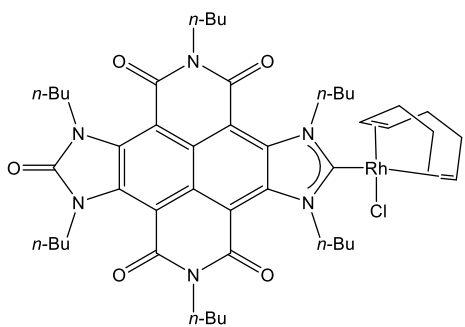
Synthesis of 2a. Complex 2a was obtained by reacting [1a](BF₄)₂ (100 mg, 0.08 mmol,



1 equiv.), [RhCl(cod)]₂ (19.72 mg, 0.04 mmol, 0.5 equiv.) and *t*BuOK (20.2 mg, 0.18 mmol, 2.2 equiv.) in THF (10 mL). After purification by column chromatography using CH₂Cl₂ as eluent, complex 2a (75 mg, 70%) was isolated as an orange oil. ¹H NMR (400 MHz, CDCl₃): δ 6.32-

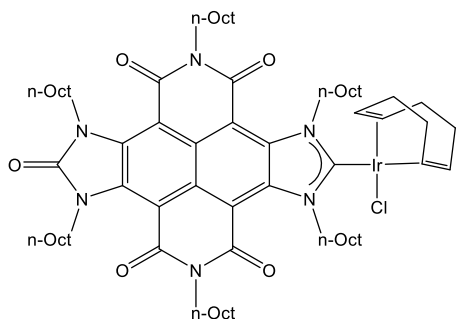
6.15 (m, 2H, CH₂ Im octyl), 5.36-5.30 (m, 2H, CH₂ Im octyl), 5.29-5.23 (br, 2H, CH_{cod}), 4.67-4.48 (m, 4H, CH₂ Im octyl), 4.33-4.21 (m, 2H, CH₂ naphth octyl), 4.12-4.02 (m, 2H, CH₂ naphth octyl), 3.63-3.49 (br, 2H, CH_{cod}), 2.62-2.41 (m, 4H, CH₂ cod), 2.15- 2.03 (m, 4H, CH₂ cod), 1.89-1.65 (m, 8H, CH₂ octyl), 1.52-1.10 (m, 64H, CH₂ octyl), 0.93-0.79 (m, 18H, CH₃ octyl). ¹³C{¹H} NMR (75 MHz, CDCl₃): δ 214.35 (d, Rh-C_{carbene}, ¹J_{Rh-C} = 51 Hz), 162.49 (C=O_{naphth}), 162.31 (C=O_{naphth}), 157.12 (C=O_{azolone}), 136.06 (C_q naphth), 135.45 (C_q naphth), 119.05 (C_q naphth), 109.64 (C_q naphth), 106.58 (C_q naphth), 101.36 (d, Rh-CH_{cod}, ¹J_{Rh-C} = 6.23 Hz), 70.13 (d, Rh-CH_{cod}, ¹J_{Rh-C} = 13.95 Hz), 53.41 (CH₂ Im octyl), 45.54 (CH₂ Im octyl), 42.11 (CH₂ naphth octyl), 33.03 (CH₂ cod), 32.07 (CH₂ octyl), 31.98 (CH₂ octyl), 31.84 (CH₂ octyl), 29.84 (CH₂ octyl), 29.59 (CH₂ octyl), 29.51 (CH₂ octyl), 29.45 (CH₂ octyl), 29.37 (CH₂ octyl), 29.32 (CH₂ octyl), 29.10 (CH₂ cod), 28.61 (CH₂ octyl), 28.25 (CH₂ octyl), 27.67 (CH₂ octyl), 27.39 (CH₂ octyl), 26.87 (CH₂ octyl), 26.55 (CH₂ octyl), 22.82 (CH₂ octyl), 22.80 (CH₂ octyl), 22.72 (CH₂ octyl), 14.28 (CH₃ octyl), 14.22 (CH₃ octyl), 14.17 (CH₃ octyl). IR (KBr): ν 1736 cm⁻¹ (C=O_{azolone}).

Synthesis of 2b. Complex 2b was obtained by reacting [1b](BF₄)₂ (100 mg, 0.11 mmol, 1 equiv.), [RhCl(cod)]₂ (27.11 mg, 0.055 mmol, 0.5 equiv.) and *t*BuOK (27.7 mg, 0.24



mmol, 2.2 equiv.) in THF (10 mL). After purification by column chromatography using CH_2Cl_2 as eluent, complex **2b** (33 mg, 30%) was isolated as an orange solid. ^1H NMR (400 MHz, CDCl_3): δ 6.32-6.19 (m, 2H, CH_2 Im butyl), 5.38-5.28 (m, 2H, CH_2 Im butyl), 5.28-5.23 (br, 2H, CH_{cod}), 4.67-4.48 (m, 4H, CH_2 Im butyl), 4.40-4.24 (m, 2H, CH_2 naphth butyl), 4.17-4.01 (m, 2H, CH_2 naphth butyl), 3.65-3.49 (br, 2H, CH_{cod}), 2.64-2.41 (m, 4H, CH_2 cod), 2.19-2.04 (m, 4H, CH_2 cod), 1.88-1.66 (m, 7H, CH_2 butyl), 1.61-1.39 (m, 17H, CH_2 butyl), 1.10-0.97 (m, 12H, CH_3 butyl), 0.88 (t, $^3J_{\text{H-H}} = 8$ Hz, 6H, CH_3 butyl). $^{13}\text{C}\{^1\text{H}\}$ NMR (100 MHz, CDCl_3): δ 214.48 (d, $\text{Rh-C}_{\text{carbene}}$, $^1J_{\text{Rh-C}} = 51$ Hz), 162.51 ($\text{C}=\text{O}_{\text{naphth}}$), 162.37 ($\text{C}=\text{O}_{\text{naphth}}$), 157.12 ($\text{C}=\text{O}_{\text{azolone}}$), 136.15 (C_{q} naphth), 135.50 (C_{q} naphth), 119.10 (C_{q} naphth), 109.68 (C_{q} naphth), 106.59 (C_{q} naphth), 101.45 (d, $\text{Rh-CH}_{\text{cod}}$, $^1J_{\text{Rh-C}} = 6$ Hz), 70.21 (d, $\text{Rh-CH}_{\text{cod}}$, $^1J_{\text{Rh-C}} = 13$ Hz), 53.25 (CH_2 Im butyl), 45.39 (CH_2 Im butyl), 41.83 (CH_2 naphth butyl), 33.04 (CH_2 cod), 30.61 (CH_2 butyl), 30.22 (CH_2 butyl), 29.74 (CH_2 butyl), 29.11 (CH_2 cod), 20.53 (CH_2 butyl), 20.00 (CH_2 butyl), 19.78 (CH_2 butyl), 13.93 (CH_3 butyl), 13.86 (CH_3 butyl), 13.79 (CH_3 butyl).

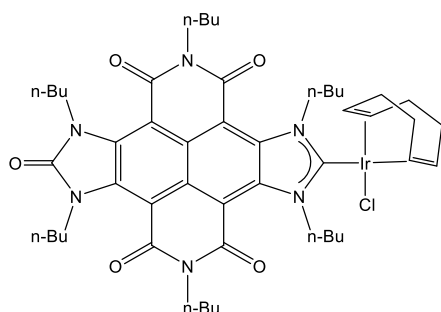
Synthesis of 3a. Complex **3a** was obtained by reacting [**1a**](BF_4)₂ (100 mg, 0.08 mmol, 1



equiv.), [$\text{IrCl}(\text{cod})_2$] (26.9 mg, 0.04 mmol, 0.5 equiv.) and *t*BuOK (20.2 mg, 0.18 mmol, 2.2 equiv.) in THF (10 mL). After purification by column chromatography using 1:4 hexane/ CH_2Cl_2 as eluent, complex **3a** (59.6 mg, 52%) was isolated as a dark pink oil. ^1H NMR (400 MHz, CDCl_3): δ 6.05-5.85 (m, 2H, CH_2 Im octyl), 5.28-5.15 (m, 2H, CH_2 Im octyl), 4.99-4.85 (m, 2H, CH_{cod}), 4.69-4.48 (m, 4H, CH_2 Im octyl), 4.36-4.22 (m, 2H, CH_2 naphth octyl), 4.14-3.99 (m, 2H, CH_2 naphth octyl), 3.22-3.09 (m, 2H, CH_{cod}), 2.45-2.25 (m, 4H, CH_2 cod), 2.01-1.61 (m, 12H, CH_2 cod and CH_2 octyl), 1.53-1.10 (m, 60H, CH_2 octyl), 0.96-0.77 (m, 18H, CH_3 octyl). $^{13}\text{C}\{^1\text{H}\}$ NMR (100 MHz, CDCl_3): δ 206.90 ($\text{Ir-C}_{\text{carbene}}$), 162.50 ($\text{C}=\text{O}_{\text{naphth}}$), 162.37 ($\text{C}=\text{O}_{\text{naphth}}$), 157.15 ($\text{C}=\text{O}_{\text{azolone}}$), 136.16 (C_{q} naphth), 135.94 (C_{q} naphth), 119.19 (C_{q} naphth), 109.68 (C_{q} naphth), 106.63 (C_{q} naphth), 88.68 (CH_{cod}), 54.31 (CH_{cod}), 53.03 (CH_2 Im octyl), 45.56 (CH_2 Im octyl), 42.13 (CH_2 naphth octyl), 33.71 (CH_2 cod), 32.04 (CH_2 octyl), 31.98 (CH_2 octyl), 31.85 (CH_2 octyl), 29.85 (CH_2 octyl), 29.62 (CH_2 octyl), 29.51 (CH_2 octyl), 29.45 (CH_2 octyl), 29.32 (CH_2 octyl), 29.30 (CH_2 octyl), 29.28 (CH_2 cod), 28.63 (CH_2 octyl),

28.14 (CH_2 octyl), 27.70 (CH_2 octyl), 27.39 (CH_2 octyl), 26.72 (CH_2 octyl), 56.57 (CH_2 octyl), 22.80 (CH_2 octyl), 22.80 (CH_2 octyl), 22.72 (CH_2 octyl), 14.26 (CH_3 octyl), 14.21 (CH_3 octyl), 14.16 (CH_3 octyl).

Synthesis of 3b. Complex **3b** was obtained by reacting [**1b**](BF_4)₂ (100 mg, 0.11 mmol,

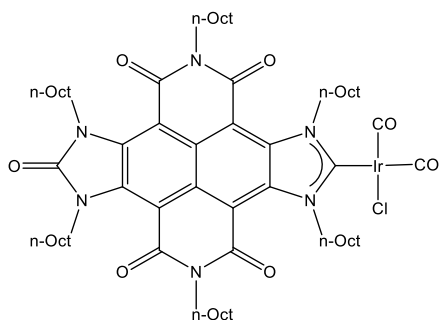


1 equiv.), [$\text{IrCl}(\text{cod})_2$] (36.9 mg, 0.055 mmol, 0.5 equiv.) and *t*BuOK (27.7 mg, 0.24 mmol, 2.2 equiv.) in THF (10 mL). After purification by column chromatography using 1:4 hexane/ CH_2Cl_2 as eluent, complex **3b** (25.3 mg, 21%) was isolated as a dark pink solid. ^1H NMR (400 MHz, CDCl_3): δ 6.06-5.88

(m, 2H, CH_2 Im butyl), 5.33-5.19 (m, 2H, CH_2 Im butyl), 4.99-4.85 (m, 2H, CH_{cod}), 4.71-4.48 (m, 4H, CH_2 Im butyl), 4.40-4.24 (m, 2H, CH_2 napht butyl), 4.17-4.01 (m, 2H, CH_2 napht butyl), 3.25-3.08 (m, 2H, CH_{cod}), 2.47-2.24 (m, 4H, CH_2 cod), 2.02-1.59 (m, 12H, CH_2 cod; CH_2 butyl), 1.59-1.36 (m, 16H, CH_2 butyl), 1.03 (t, $^3J_{\text{H-H}} = 8$ Hz, 6H, CH_3 butyl), 0.97 (t, $^3J_{\text{H-H}} = 8$ Hz, 6H, CH_3 butyl), 0.89 (t, $^3J_{\text{H-H}} = 8$ Hz, 6H, CH_3 butyl). $^{13}\text{C}\{^1\text{H}\}$ NMR (100 MHz, CDCl_3): δ 206.95 (Ir- $\text{C}_{\text{carbine}}$), 162.52 ($\text{C}=\text{O}_{\text{napht}}$), 162.42 ($\text{C}=\text{O}_{\text{napht}}$), 157.14 ($\text{C}=\text{O}_{\text{azolone}}$), 136.17 (C_{q} napht), 135.99 (C_{q} napht), 119.22 (C_{q} napht), 109.70 (C_{q} napht), 106.63 (C_{q} napht), 88.76 (CH_{cod}), 54.39 (CH_{cod}), 52.84 (CH_2 Im butyl), 45.37 (CH_2 Im butyl), 41.84 (CH_2 napht butyl), 33.71 (CH_2 cod), 30.63 (CH_2 butyl), 30.13 (CH_2 butyl), 29.85 (CH_2 butyl), 29.62 (CH_2 cod), 20.53 (CH_2 butyl), 19.88 (CH_2 butyl), 19.79 (CH_2 butyl), 14.25 (CH_3 butyl), 13.93 (CH_3 butyl), 13.80 (CH_3 butyl).

Carbonyl Derivatives. General Procedure. CO gas (1 atm, 10 mL/min) was passed through a solution of complexes **3a** or **3b** (20 mg) in dichloromethane (10 mL) for 45 minutes at 0 °C. An immediate colour change from dark pink or red to yellow was observed. The solvent was removed under reduced pressure, giving the desired carbonyl derivative in high yields (90-99%).

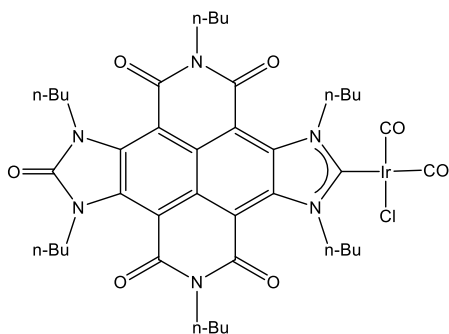
Synthesis of 4a. Compound **4a** was prepared starting from **3a** (20 mg, 14.6 mmol).



Following the general procedure, **4a** (17.3 mg, 90%) was isolated as a yellowish oil. ^1H NMR (300 MHz, CDCl_3): δ 5.53-5.30 (m, 4H, CH_2 Im octyl), 4.64-4.52 (m, 4H, CH_2 Im octyl), 4.28-4.09 (m, 4H, CH_2 napht octyl), 1.87-1.66 (m, 8H, CH_2 octyl), 1.53-1.12 (m, 64H, CH_2 octyl), 0.92-0.80 (m, 18H, CH_3 octyl). $^{13}\text{C}\{^1\text{H}\}$ NMR

(75 MHz, CDCl₃): δ 194.95 (Ir-C_{carbene}), 180.4717 (C=O_{Ir}) 167.96 (C=O_{Ir}), 162.18 (C=O_{napht}), 162.08 (C=O_{napht}), 157.02 (C=O_{azolone}), 135.00 (C_{q napht}), 134.59 (C_{q napht}), 120.29 (C_{q napht}), 112.07 (C_{q napht}), 106.12 (C_{q napht}), 54.18 (CH_{2 Im octyl}), 45.62 (CH_{2 Im octyl}), 42.24 (CH_{2 napht octyl}), 31.97 (CH_{2 octyl}), 31.93 (CH_{2 octyl}), 31.85 (CH_{2 octyl}), 29.85 (CH_{2 octyl}), 29.48 (CH_{2 octyl}), 29.44 (CH_{2 octyl}), 29.36 (CH_{2 octyl}), 29.32 (CH_{2 octyl}), 29.28 (CH_{2 octyl}), 28.80 (CH_{2 cod}), 28.61 (CH_{2 octyl}), 27.59 (CH_{2 octyl}), 27.35 (CH_{2 octyl}), 26.59 (CH_{2 octyl}), 26.55 (CH_{2 octyl}), 22.84 (CH_{2 octyl}), 22.80 (CH_{2 octyl}), 22.73 (CH_{2 octyl}), 14.26 (CH_{3 octyl}), 14.22 (CH_{3 octyl}), 14.17 (CH_{3 octyl}). IR (CH₂Cl₂): 1739 (v_{C=O azolone}), 1990 (v_{Ir-CO}) and 2072 (v_{Ir-CO}) cm⁻¹.

Synthesis of 4b. Compound **4b** was prepared starting from **3b** (20 mg, 19.3 mmol).



Following the general procedure, **4b** (18.8 mg, 99%) was isolated as a yellowish solid. ¹H NMR (300 MHz, CDCl₃): δ 5.62-5.27 (m, 4H, CH_{2 Im butyl}), 4.69-4.50 (m, 4H, CH_{2 Im butyl}), 4.34-4.09 (m, 4H, CH_{2 napht butyl}), 1.88-1.63 (m, 8H, CH_{2 butyl}), 1.63-1.40 (m, 16H, CH_{2 butyl}), 1.08-0.87 (m, 18H, CH_{3 butyl}). ¹³C {¹H} NMR (75 MHz, CDCl₃): δ 194.97

(Ir-C_{carbene}), 180.46 (C=O_{Ir}) 167.92 (C=O_{Ir}), 162.19 (C=O_{napht}), 162.11 (C=O_{napht}), 156.99 (C=O_{azolone}), 137.03 (C_{q napht}), 134.60 (C_{q napht}), 120.30 (C_{q napht}), 112.08 (C_{q napht}), 106.10 (C_{q napht}), 53.98 (CH_{2 Im butyl}), 45.41 (CH_{2 Im butyl}), 41.96 (CH_{2 napht butyl}), 30.77 (CH_{2 butyl}), 30.60 (CH_{2 butyl}), 29.61 (CH_{2 butyl}), 20.49 (CH_{2 butyl}), 19.82 (CH_{2 butyl}), 19.77 (CH_{2 butyl}), 13.92 (CH_{3 butyl}), 13.89 (CH_{3 butyl}), 13.78 (CH_{3 butyl}). IR (CH₂Cl₂): 1739 (v_{C=O azolone}), 1991 (v_{Ir-CO}) and 2072 (v_{Ir-CO}) cm⁻¹.

3. Spectroscopic data

3.1. ^1H and ^{13}C spectra of Ib in CDCl_3

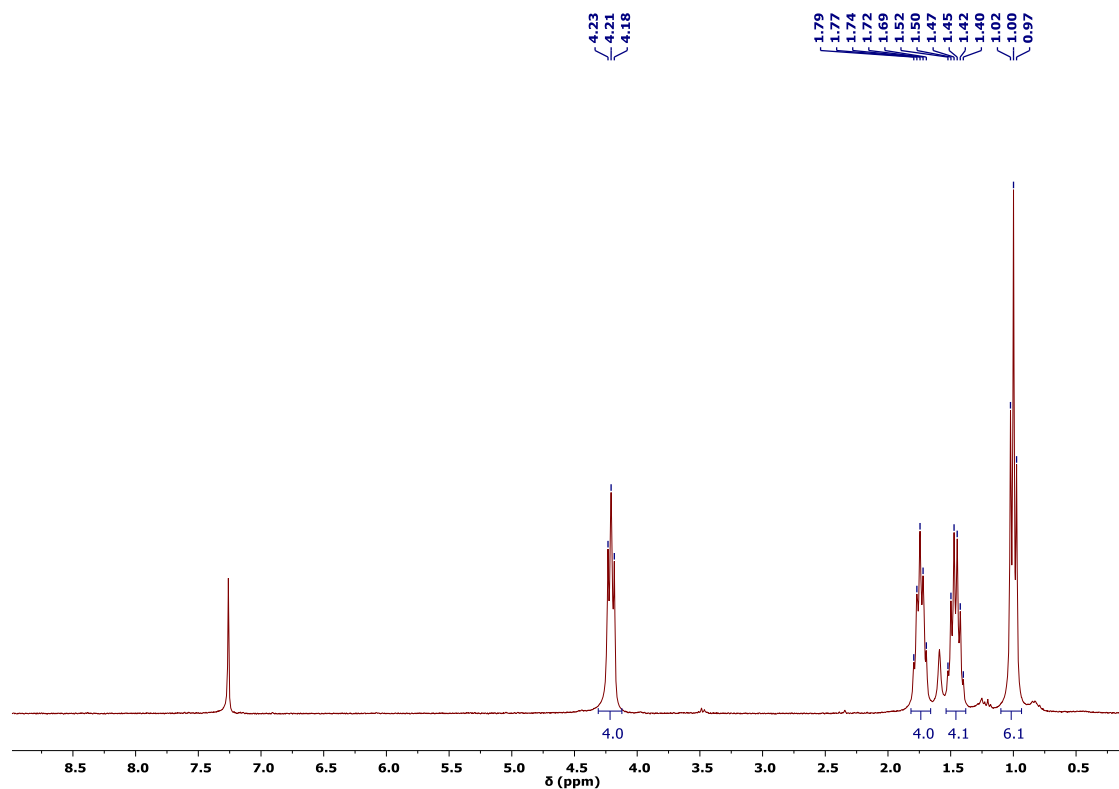


Figure S1. ^1H NMR spectrum (300 MHz, CDCl_3) of **Ib**

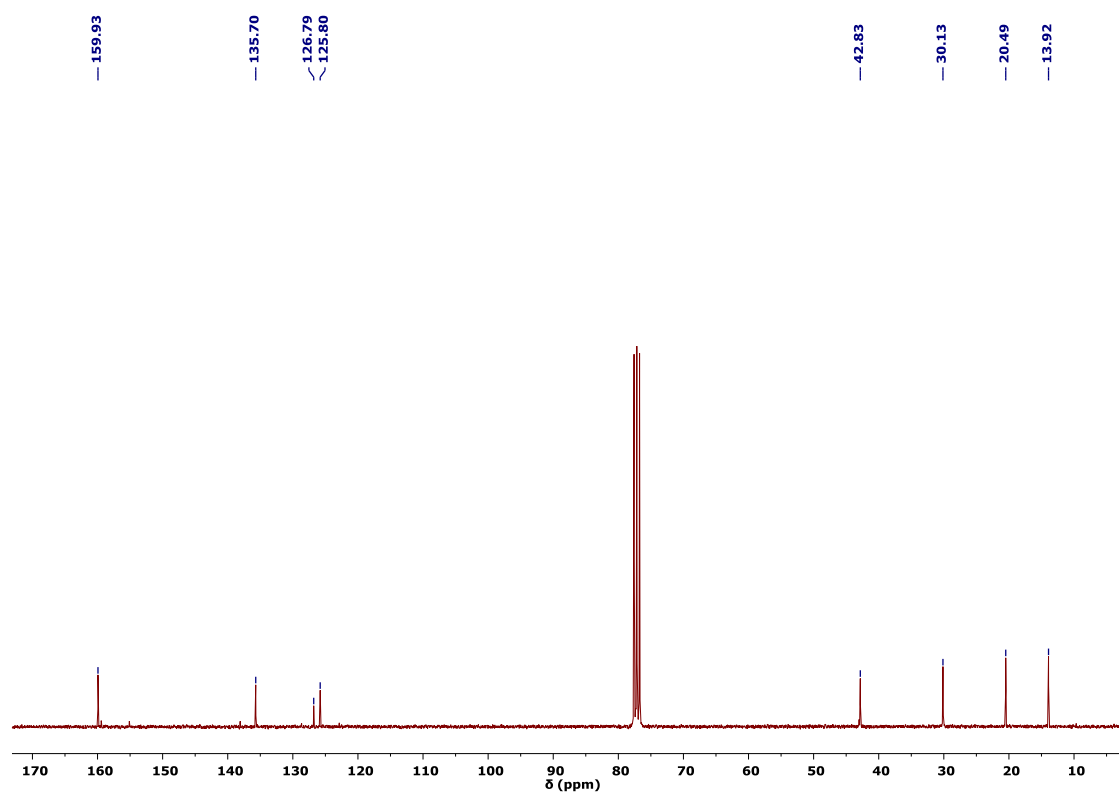


Figure S2. $^{13}\text{C}\{^1\text{H}\}$ spectrum (75 MHz, CDCl_3) of **Ib**

3.2. ^1H , ^{13}C and HSQC spectra of $[\mathbf{1a}](\text{BF}_4)_2$ in CDCl_3

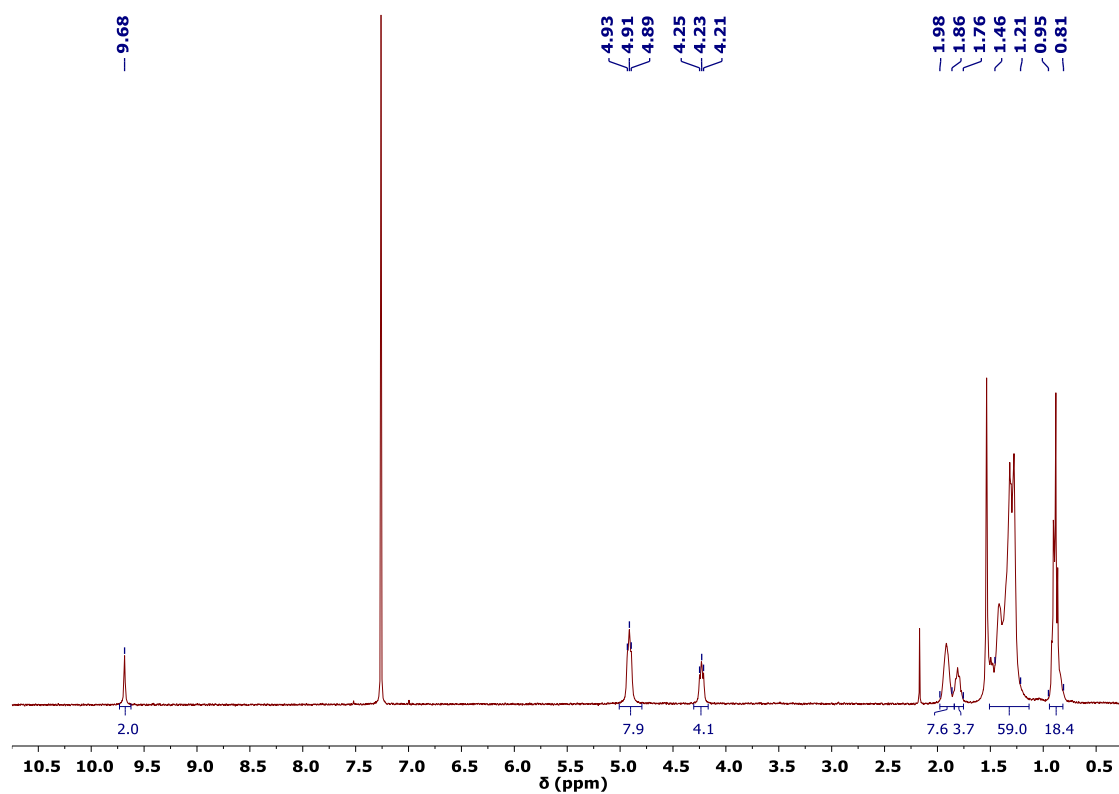


Figure S3. ^1H NMR spectrum (400 MHz, CDCl_3) of $[\mathbf{1a}](\text{BF}_4)_2$

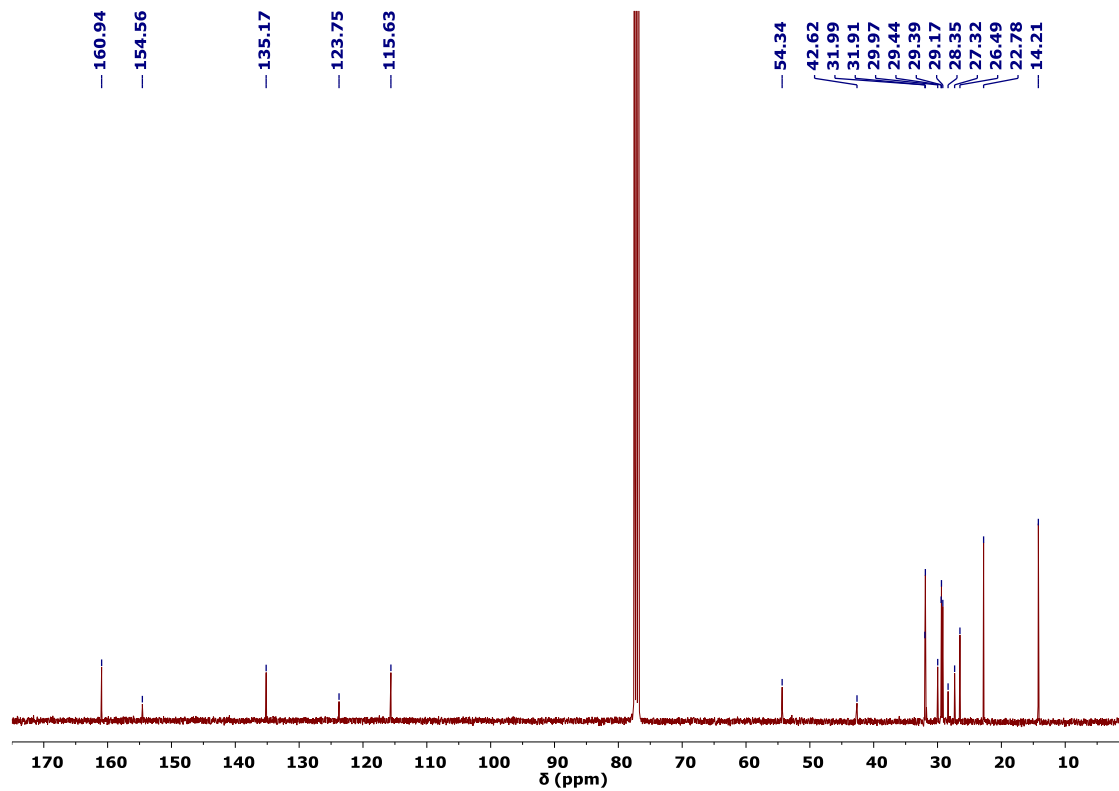


Figure S4. $^{13}\text{C}\{^1\text{H}\}$ spectrum (100 MHz, CDCl_3) of $[\mathbf{1a}](\text{BF}_4)_2$

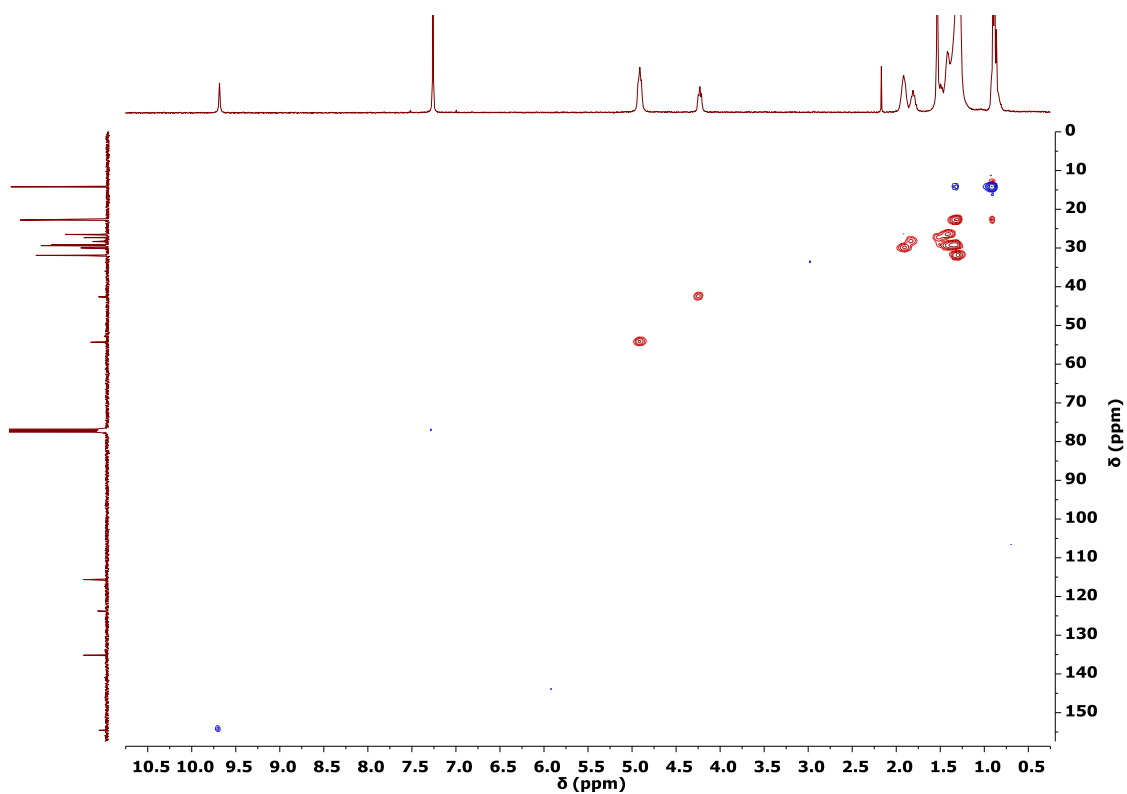


Figure S5. ^1H - ^{13}C HSQC spectrum (400 MHz, CDCl_3) of $[\mathbf{1a}](\text{BF}_4)_2$

3.3. ^1H , ^{13}C and HSQC spectra of $[\mathbf{1b}](\text{BF}_4)_2$ in CD_3CN

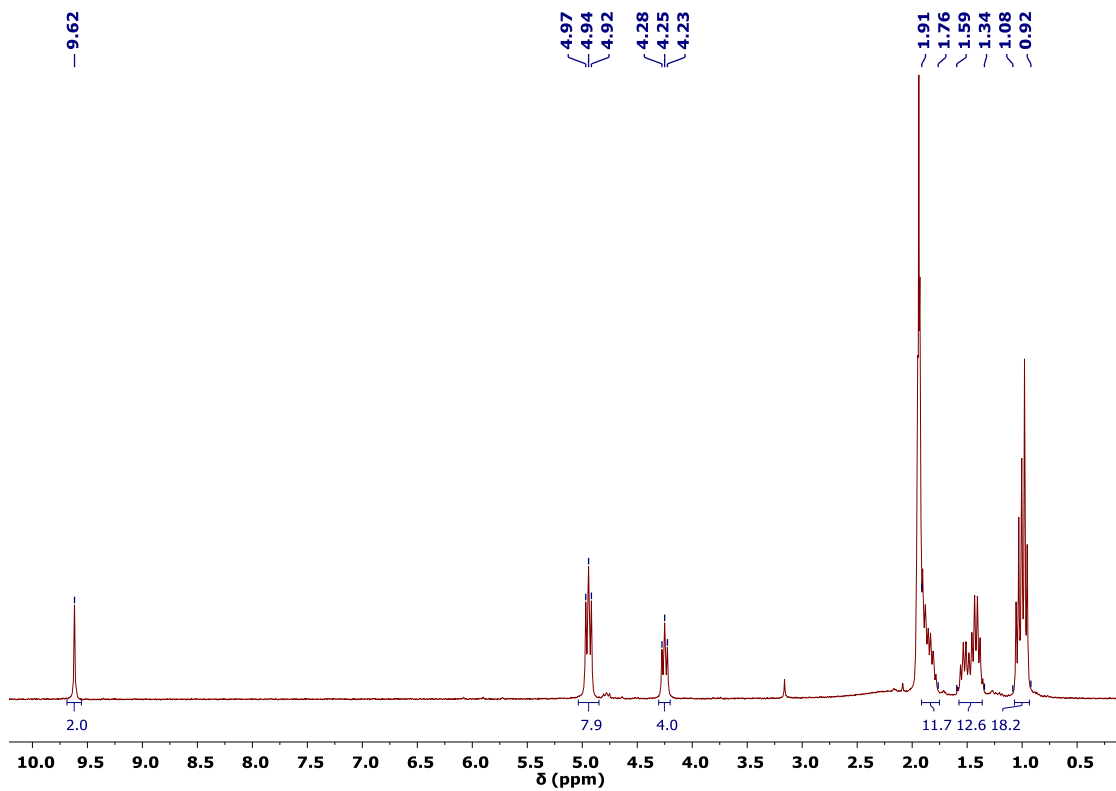


Figure S6. ^1H NMR spectrum (300 MHz, CD_3CN) of $[\mathbf{1b}](\text{BF}_4)_2$

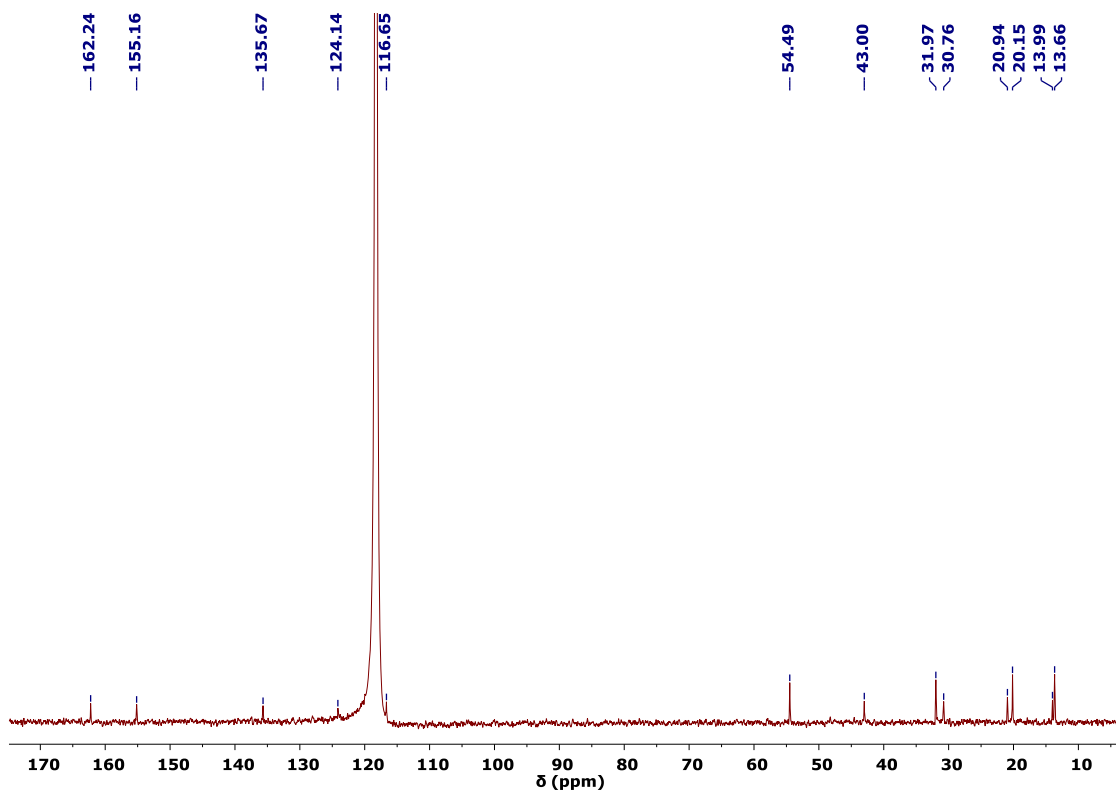


Figure S7. $^{13}\text{C}\{^1\text{H}\}$ spectrum (75 MHz, CD_3CN) of $[\mathbf{1b}](\text{BF}_4)_2$

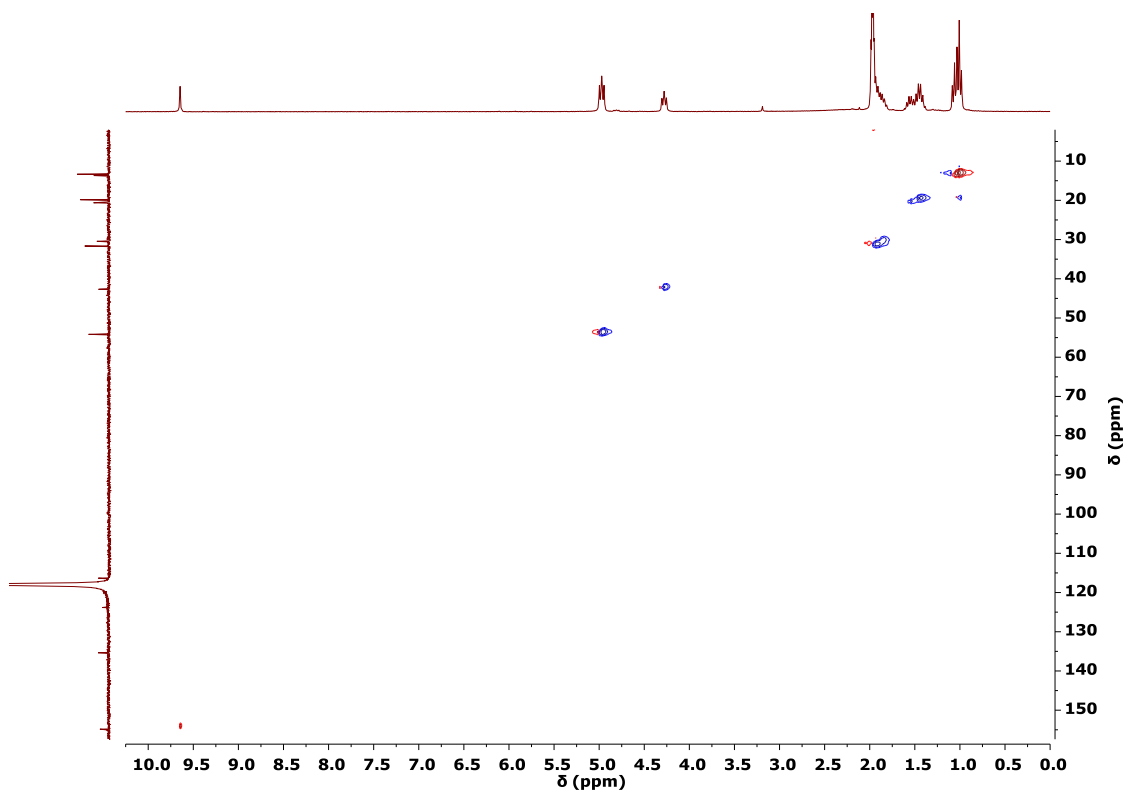


Figure S8. $^1\text{H}-^{13}\text{C}$ HSQC spectrum (300 MHz, CD_3CN) of $[\mathbf{1b}](\text{BF}_4)_2$

3.4. ^1H , ^{13}C , HSQC and HMBC spectra of 2a in CDCl_3

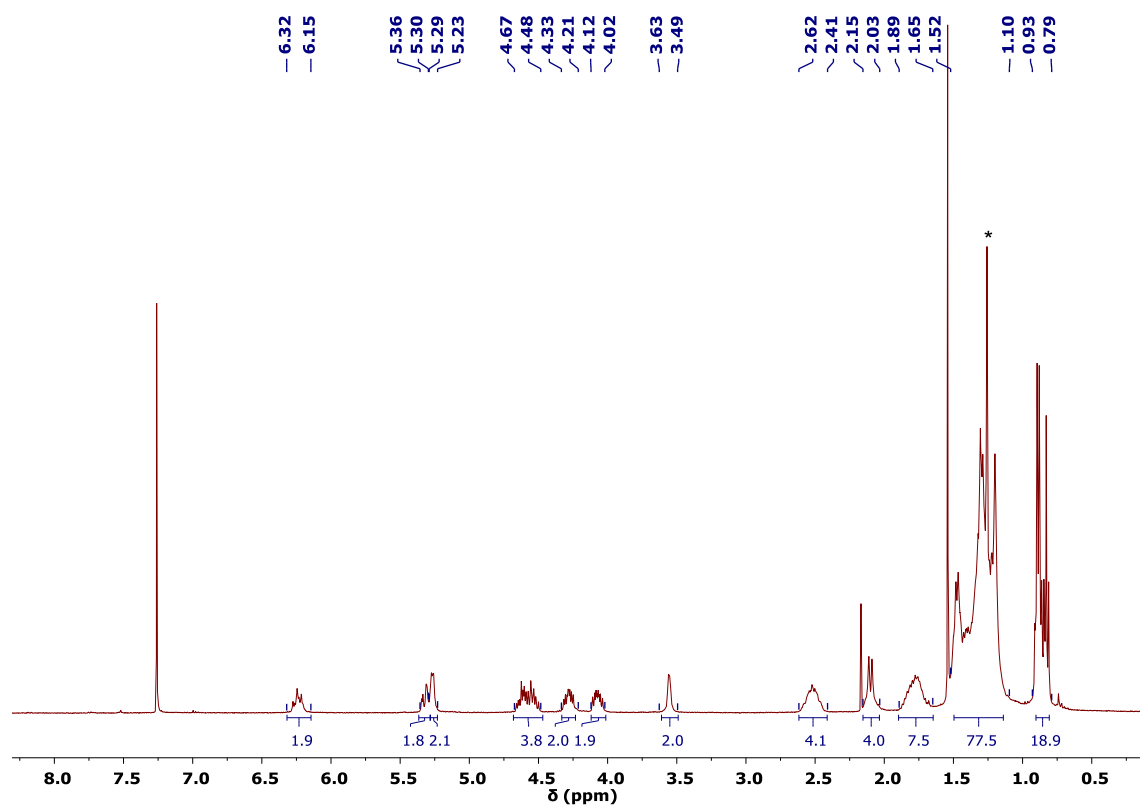


Figure S9. ^1H NMR spectrum (400 MHz, CDCl_3) of 2a

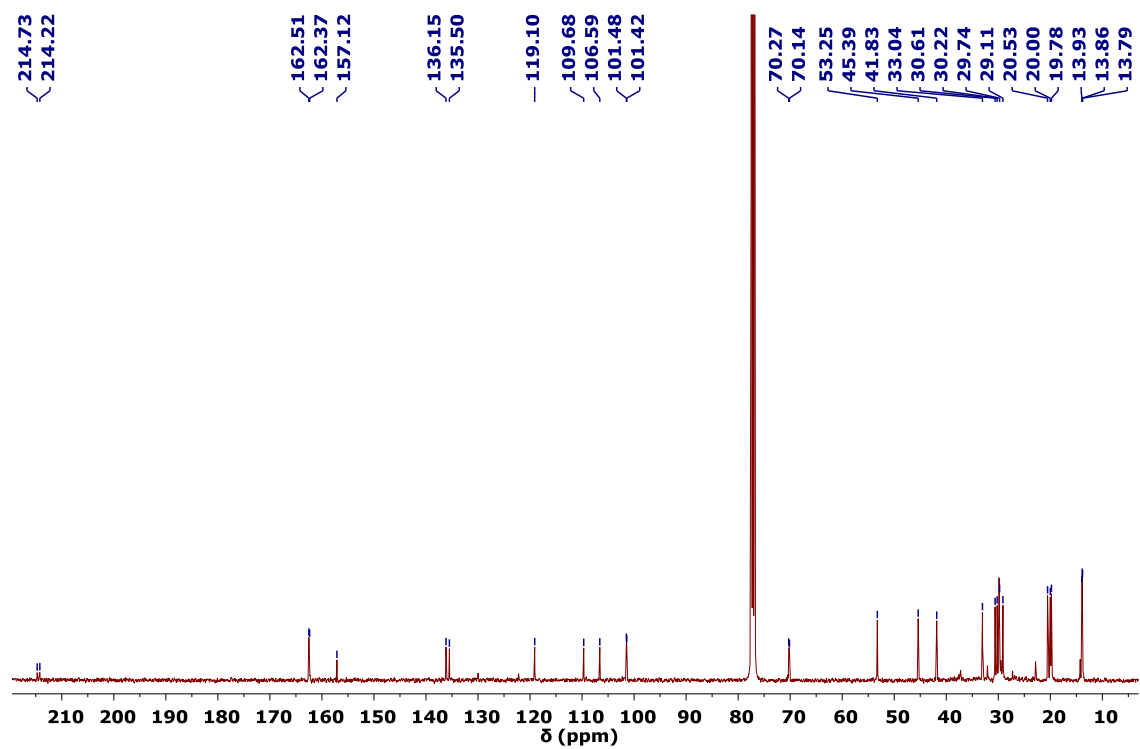


Figure S10. $^{13}\text{C}\{^1\text{H}\}$ spectrum (75 MHz, CDCl_3) of 2a

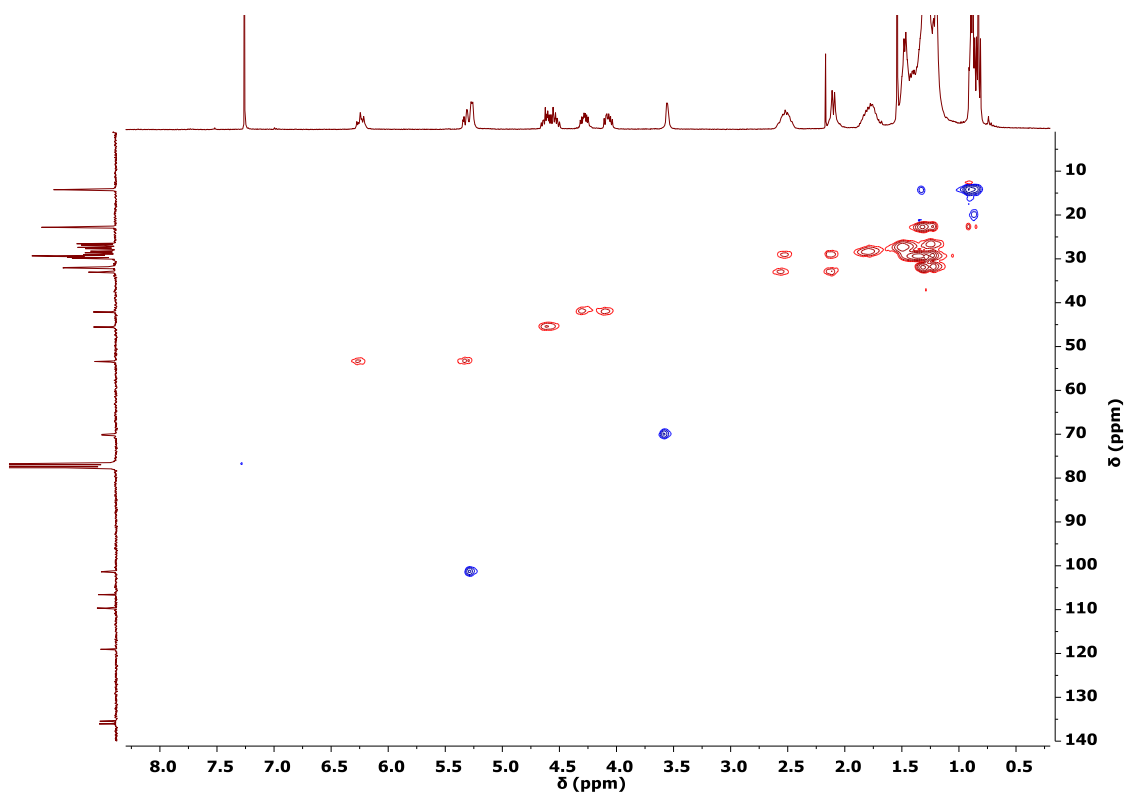


Figure S11. ^1H - ^{13}C HSQC spectrum (300 MHz, CDCl_3) of **2a**

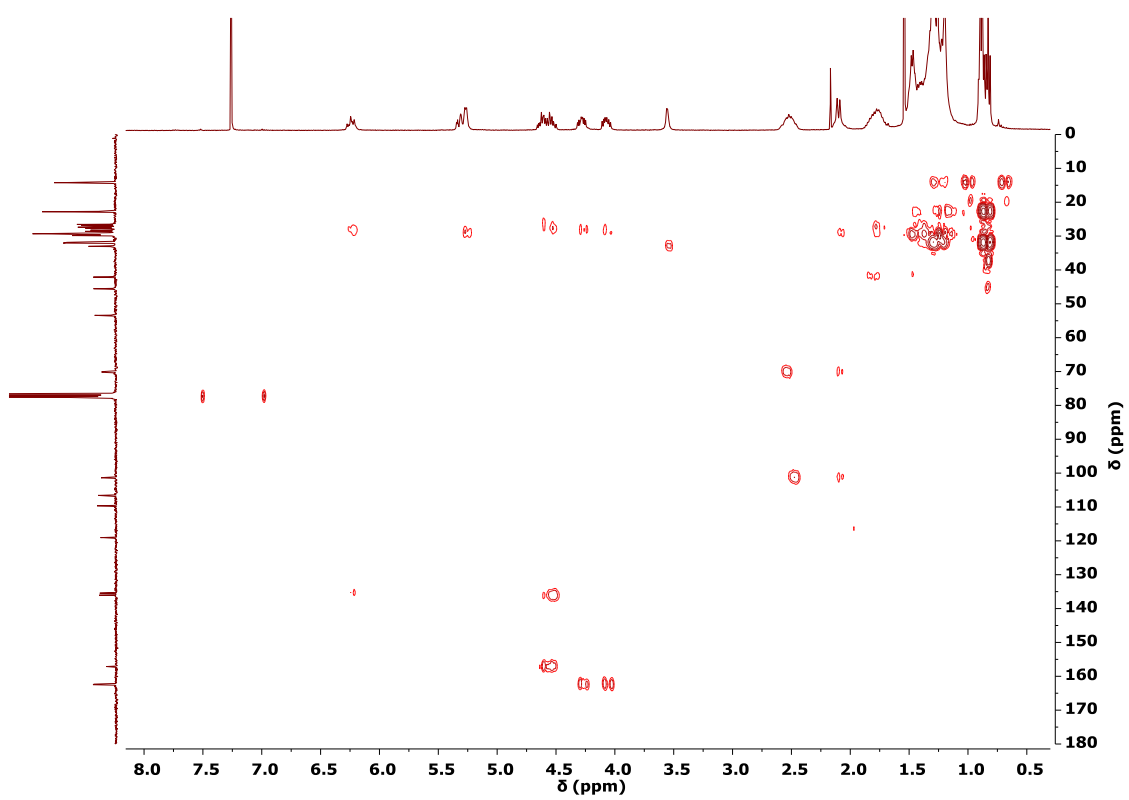


Figure S12. ^1H - ^{13}C HMBC spectrum (300 MHz, CDCl_3) of **2a**

3.5. ^1H , ^{13}C and HSQC spectra of 2b in CDCl_3

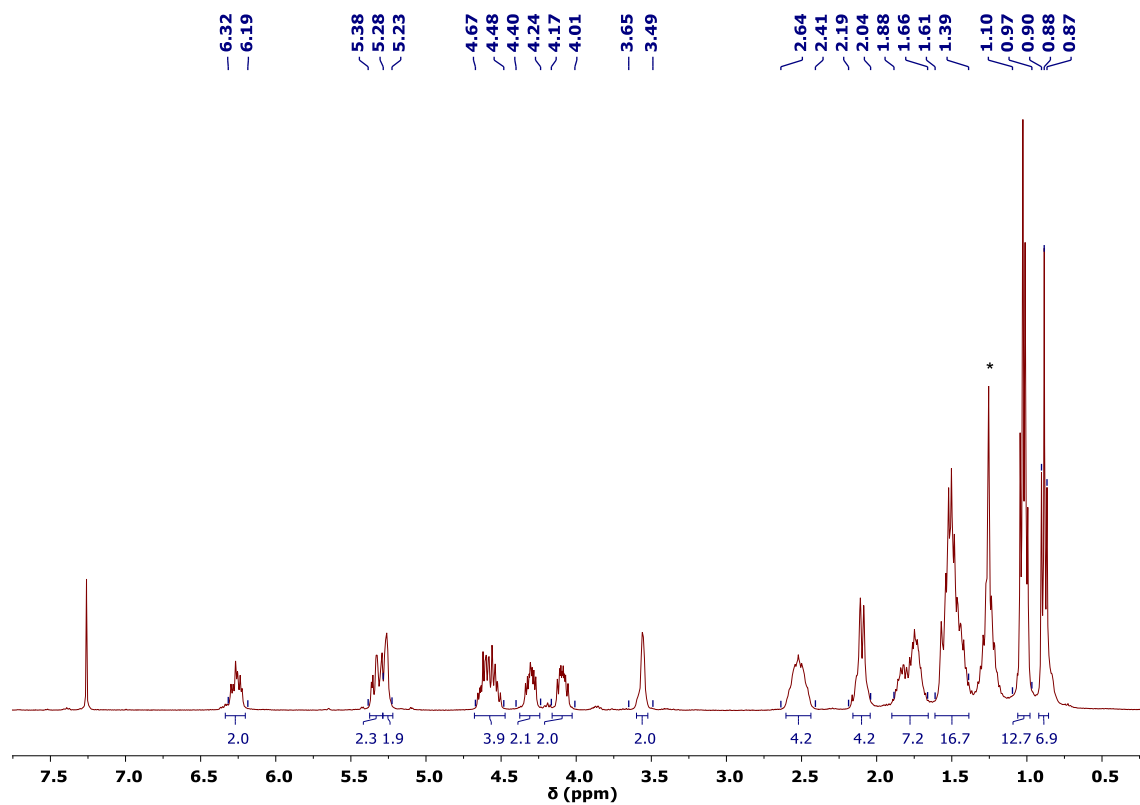


Figure S13. ^1H NMR spectrum (400 MHz, CDCl_3) of **2b**

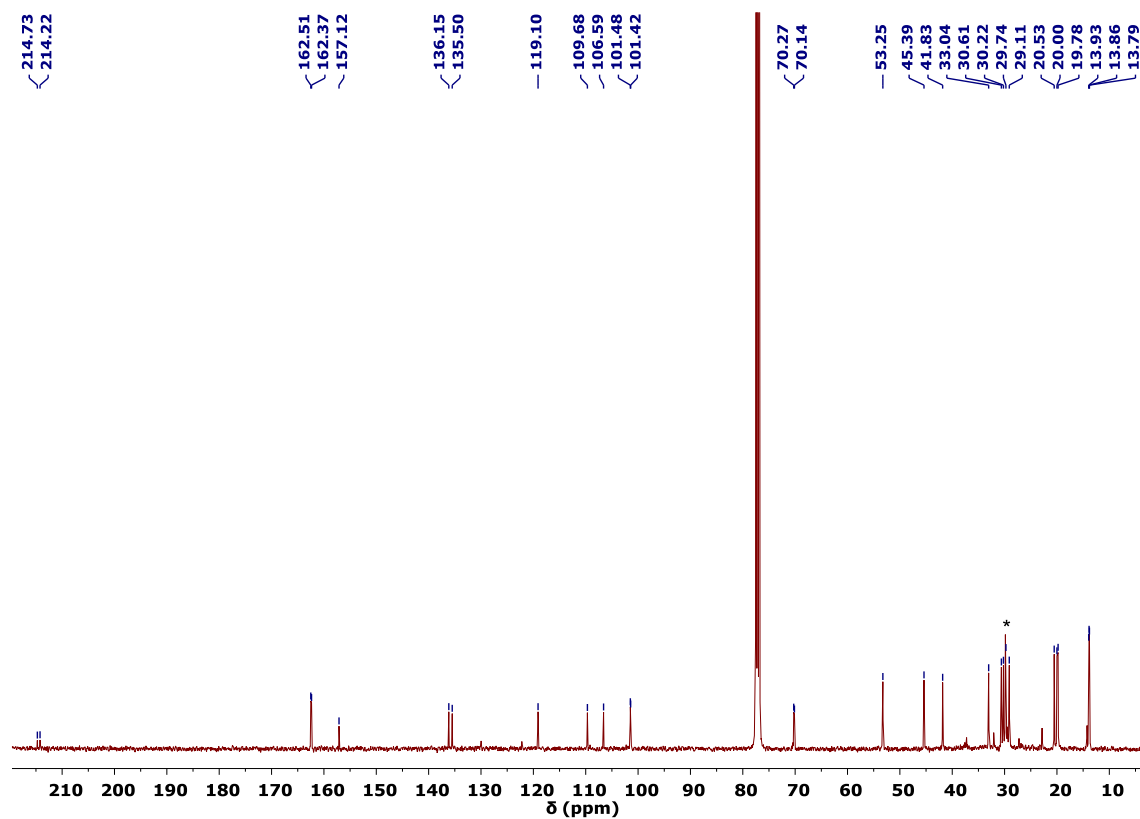


Figure S14. $^{13}\text{C}\{^1\text{H}\}$ spectrum (100 MHz, CDCl_3) of **2b**

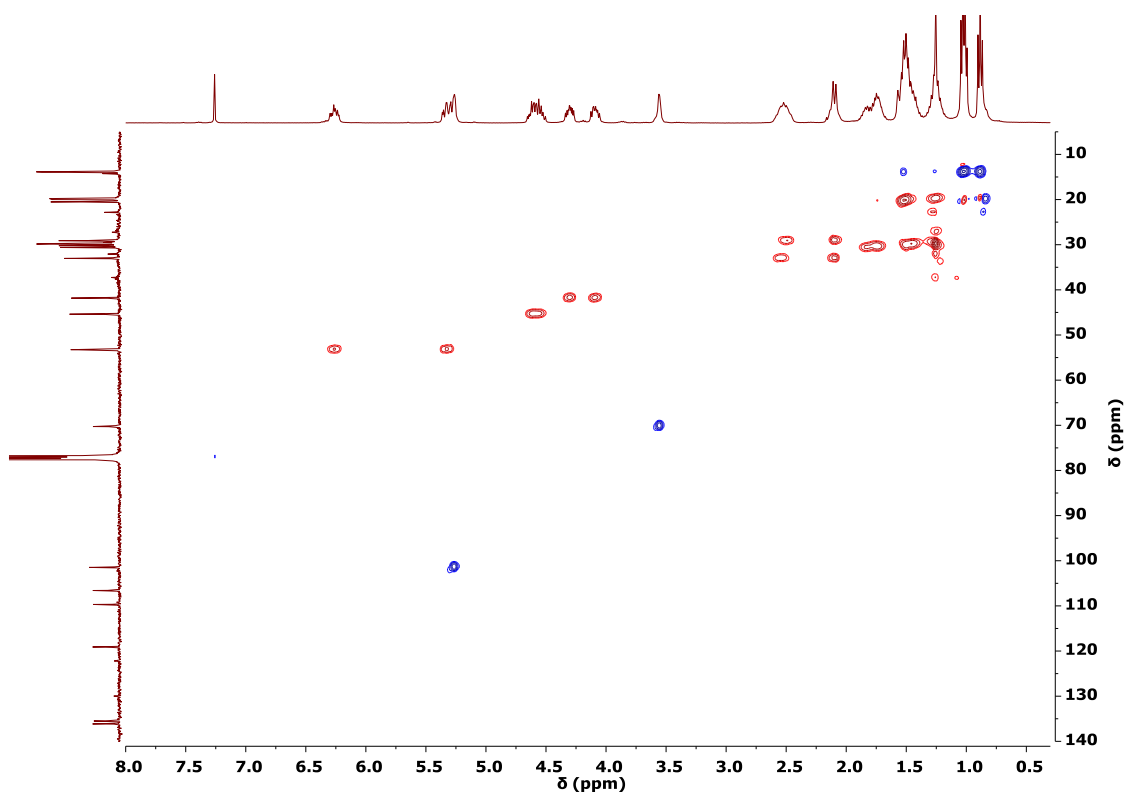


Figure S15. ^1H - ^{13}C HSQC spectrum (400 MHz, CDCl_3) of **2b**

3.6. ^1H , ^{13}C and HSQC spectra of **3a** in CDCl_3

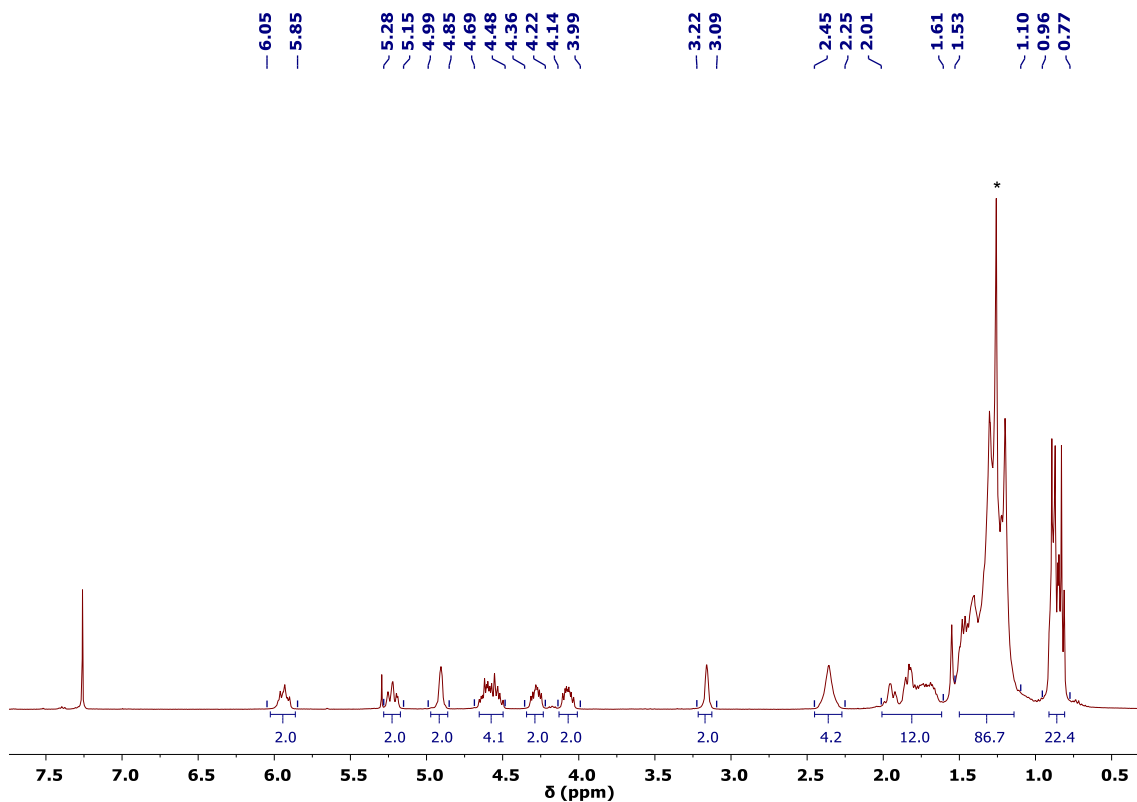


Figure S16. ^1H NMR spectrum (400 MHz, CDCl_3) of **3a**

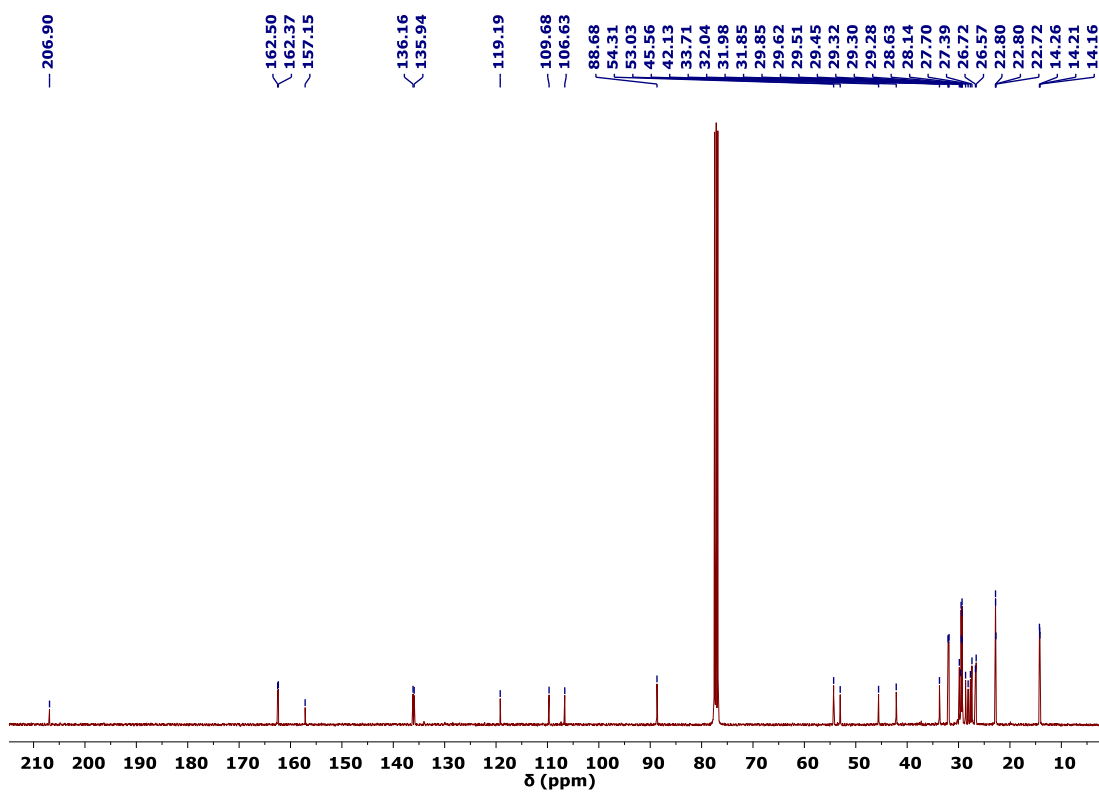


Figure S17. ^{13}C NMR spectrum (100 MHz, CDCl_3) of **3a**

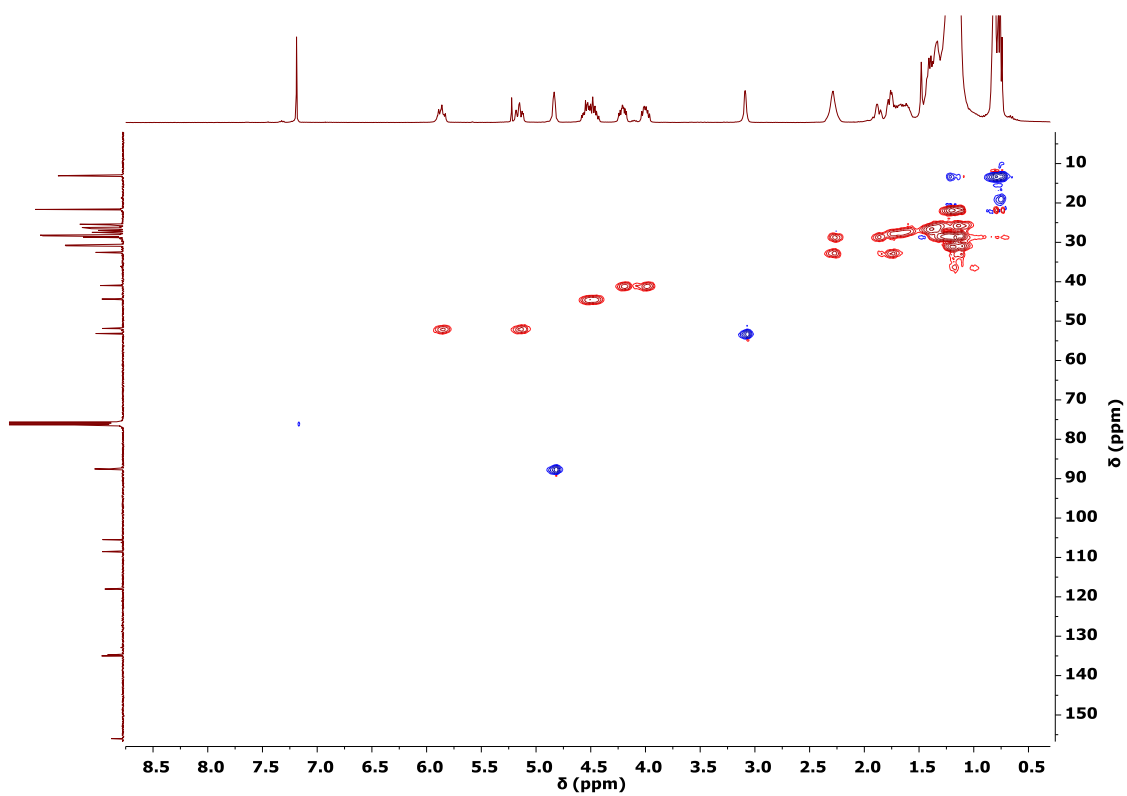


Figure S18. ^1H - ^{13}C HSQC spectrum (400 MHz, CDCl_3) of **3a**

3.7. ^1H and ^{13}C spectra of **3b** in CDCl_3

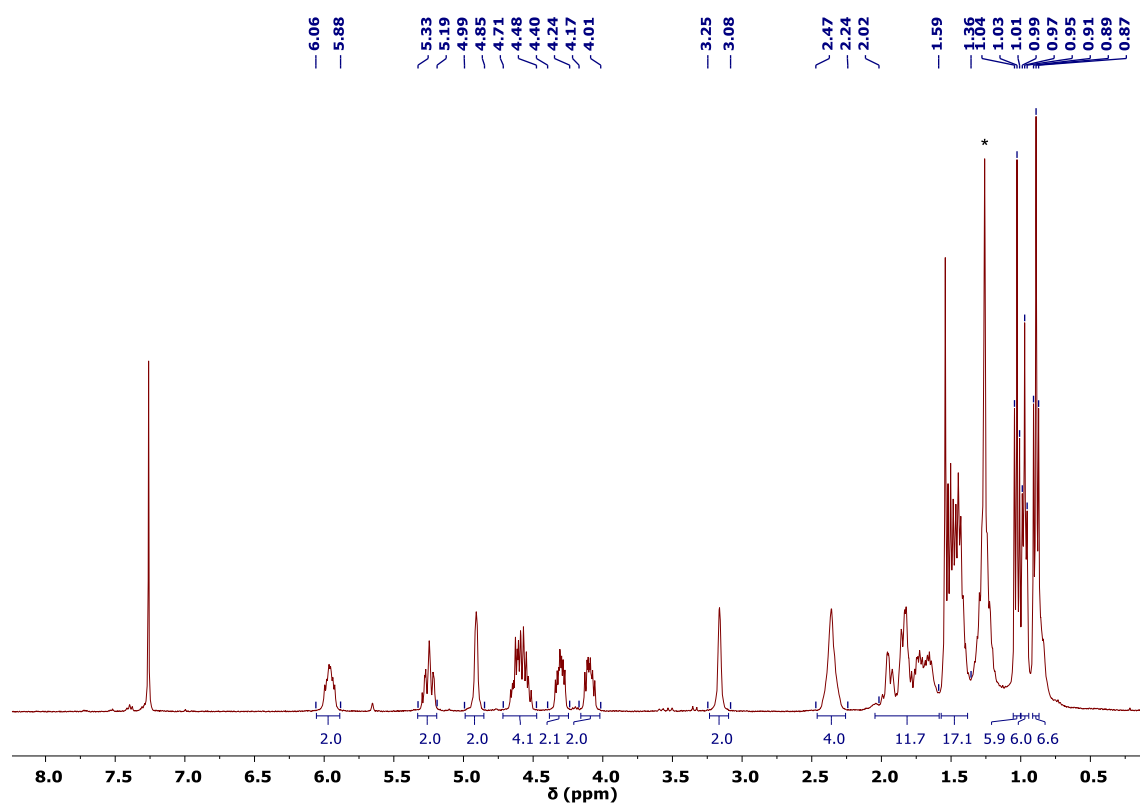


Figure S19. ^1H NMR spectrum (400 MHz, CDCl_3) of **3b**

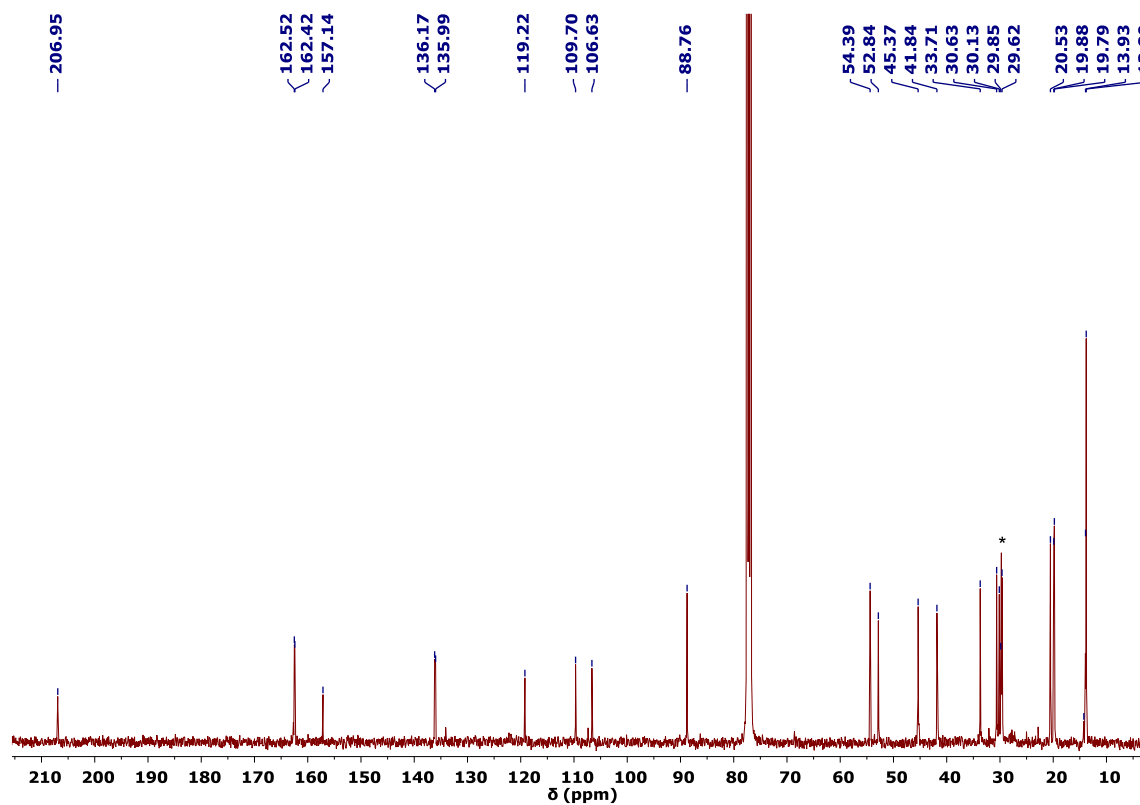


Figure S20. ^{13}C NMR spectrum (100 MHz, CDCl_3) of **3b**

3.8. ^1H and ^{13}C spectra of 4a in CDCl_3

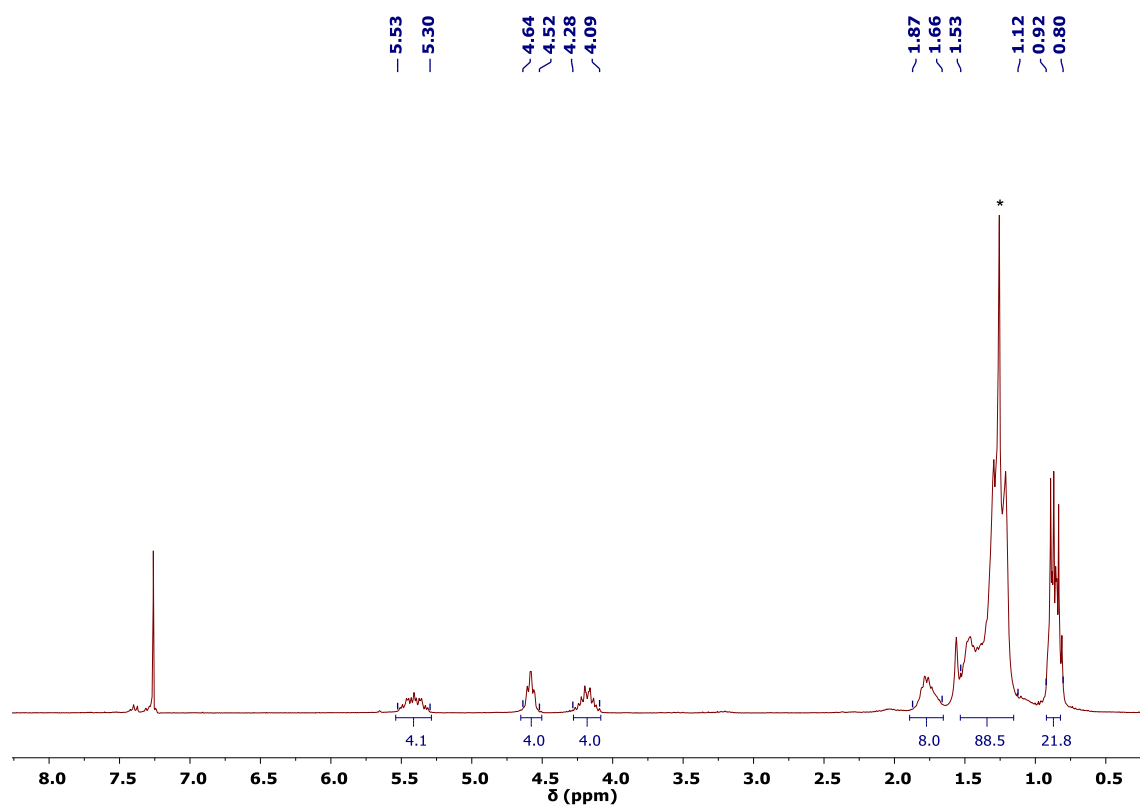


Figure S21. ^1H NMR spectrum (300 MHz, CDCl_3) of 4a

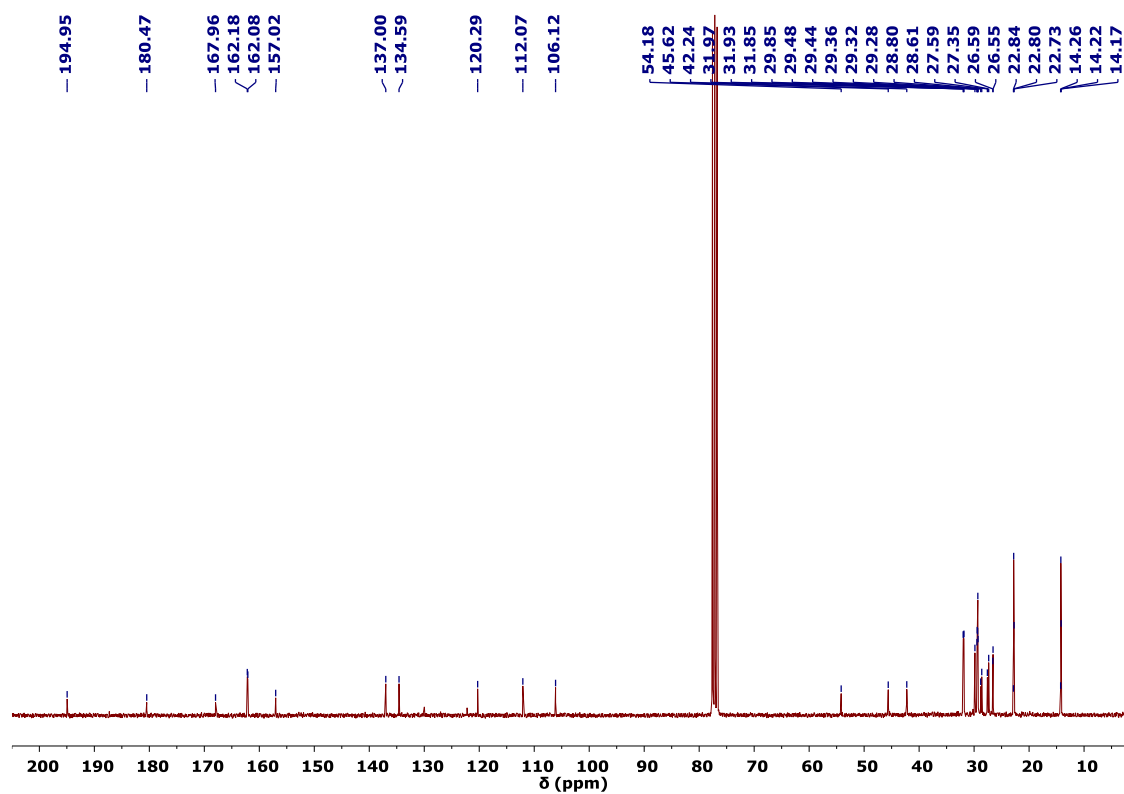


Figure S22. ^{13}C NMR spectrum (75 MHz, CDCl_3) of 4a

3.9. ^1H and ^{13}C spectra of **4b** in CDCl_3

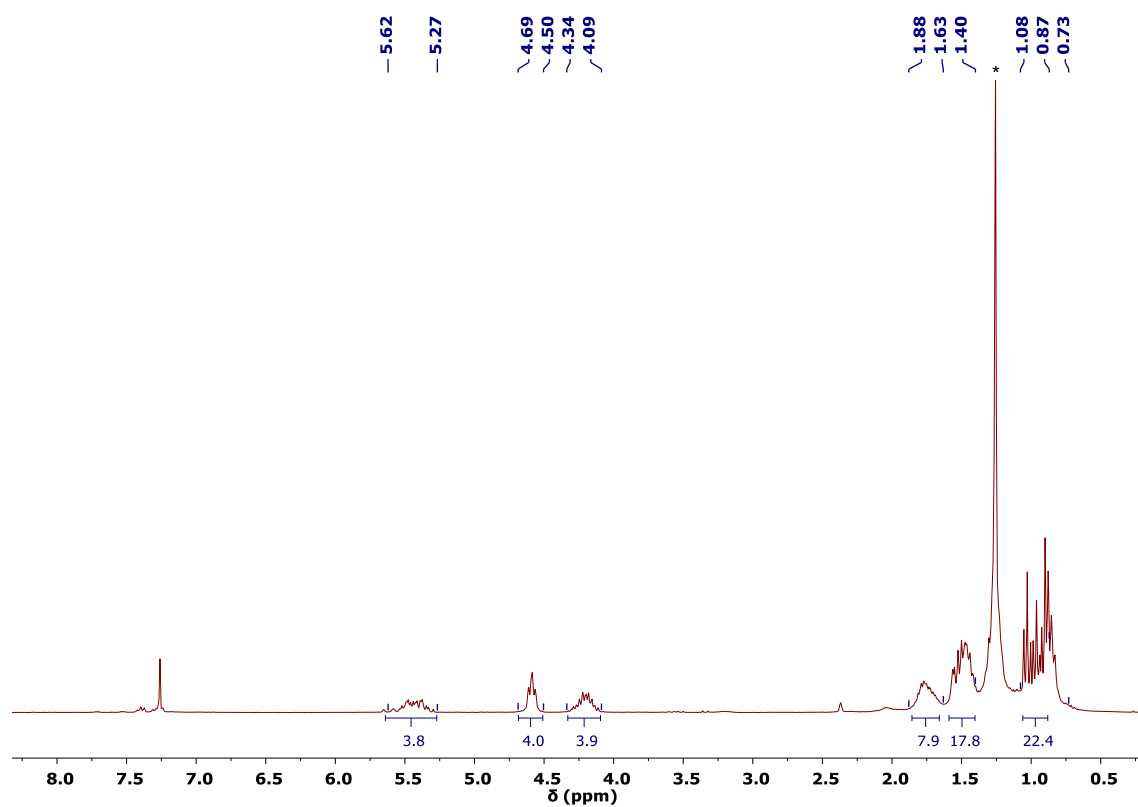


Figure S23. ^1H NMR spectrum (300 MHz, CDCl_3) of **4b**

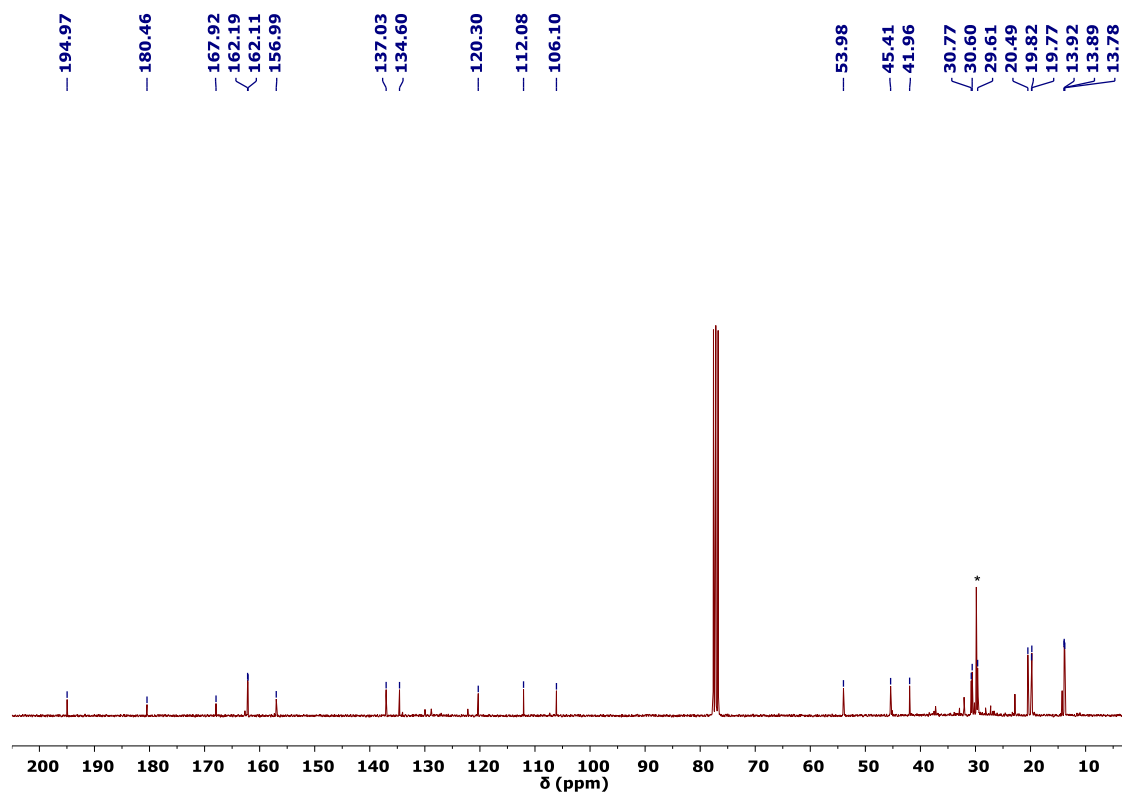


Figure S24. ^{13}C NMR spectrum (75 MHz, CDCl_3) of **4b**

4. X-Ray crystallography

X-Ray Diffraction studied for compounds [1a](BF₄)₂ and 3b. Crystals suitable for X-Ray studies of [1a](BF₄)₂ were obtained by slow evaporation of a concentrated solution of the compound in chloroform. Suitable crystals for X-Ray studies of complex 3b were obtained by slow diffusion of methanol into a concentrated solution of the complex in dichlorometane. Diffraction data was collected on an Agilent SuperNova diffractometer equipped with an Atlas CCD detector using Cu-K α radiation ($\lambda = 1.54184 \text{ \AA}$). Single crystals were mounted on a MicroMount[®] polymer tip (MiteGen) in a random orientation. Absorption corrections based on multi-scan [1a](BF₄)₂ and gaussian (3b) methods. Using Olex2,^[5] the molecular structures of the compounds were solved by direct methods using the ShelXS program or Charge Flipping in Superflip,^[6] and refined by least squares with the ShelXL refinement package.^[7] Key details of the crystals and structure refinement data are summarized in Supplementary Table S1. Further crystallographic details may be found in the CIF files, which were deposited at the Cambridge Crystallographic Data Centre, Cambridge, UK. The reference numbers for compounds [1a](BF₄)₂ and 3b were assigned as 2089245 and 2089246, respectively.

The structure model of compound [1a](BF₄)₂ exhibits significant disorder in two of the four n-octyl N-substituents. For the two disordered n-octyl chains, restraints on displacement parameters (SHELX SIMU and DELU) as well as distance restraints (DFIX) on some atoms were applied. Nevertheless, CheckCIF on Platon showed one B alert for the molecular structure of [1a](BF₄)₂:

PLAT097_ALERT_2_B Large Reported Max. (Positive) Residual Density 1.29 eA⁻³

RESPONSE The following information can be found in the shelx.lst:

Electron density synthesis with coefficients Fo-Fc

Highest peak 1.29 at 0.6462 0.1555 0.0940 [0.87 A from H55B]

This larger than expected residual electron density close to one of the carbon atoms of one of the n-octyl chains, might be caused by the disorder that we encountered in this region.

The structure model of complex **3b** also exhibits significant disorder in some of the *n*-butyl N-substituents. Restraints on displacement parameters (SHELX SIMU and DELU) as well as distance restraints (DFIX) on some atoms were applied. A global, enhanced rigid bond restrain (SHELX RIGU) was applied. Anisotropic constrains (SHELX EADP) were also used to refine the disorder. CheCIF on Platon did not show any A nor B alerts for the molecular structure of **3b**.

Figure S25 depicts two perspectives of the preliminary molecular structure of the bis-azolone isolated as the result of the oxidation of bis-imidazolium salt [**1b**](BF₄)₂. Although the data collected were not of enough quality for their publication, we decided to include this preliminary molecular structure in order to support the connectivity between atoms.

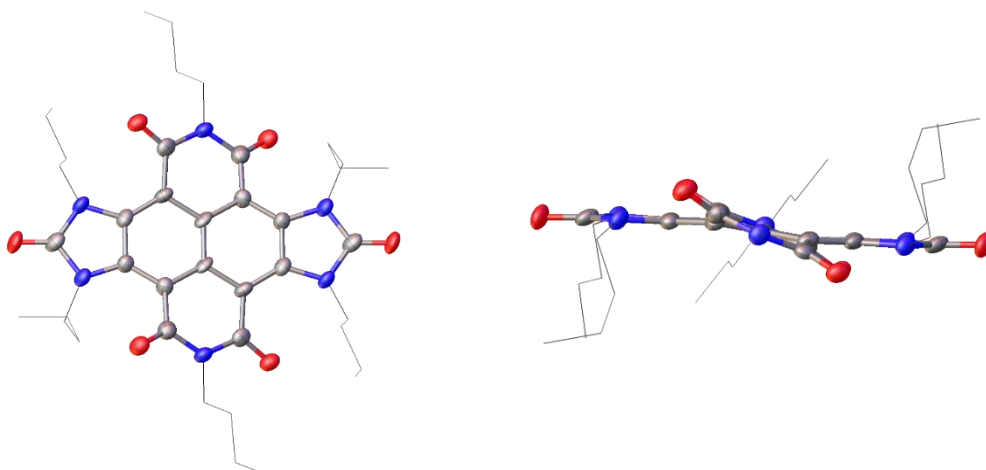


Figure S25. Two perspectives of the molecular structure of the bis-azolone, product of the oxidation of [**1b**](BF₄)₂. Ellipsoids are at 50% probability. Hydrogen atoms have been omitted for clarity. The *n*-butyl chains are represented in the wireframe form. Carbon atoms are depicted in grey, oxygen atoms in red and nitrogen atoms in light blue

Table S1. Summary of crystal data, data collection, and structure refinement details of compounds [1a](BF₄)₂ and 3b

| | [1a](BF ₄) ₂ | 3b |
|---|--|---|
| Empirical formula | C ₆₄ H ₁₀₄ N ₆ O ₄ B ₂ F ₈ | C ₄₈ H ₆₆ ClIrN ₆ O ₅ |
| Formula weight | 1195.15 | 1034.71 |
| Temperature/K | 200(14) | 200(1) |
| Crystal system | Monoclinic | Triclinic |
| Space group | P2 ₁ /n | P-1 |
| a/Å | 10.4386(2) | 16.6424(2) |
| b/Å | 15.0700(4) | 19.2577(3) |
| c/Å | 43.8508(12) | 25.1758(3) |
| α/° | 90 | 79.6470(10) |
| β/° | 95.829(2) | 89.3150(10) |
| γ/° | 2 | 68.1170(10) |
| Volume/Å³ | 6862.4(3) | 7352.04(18) |
| Z | 4 | 6 |
| ρ_{calc}/mg/mm³ | 1.157 | 1.402 |
| μ/mm⁻¹ | 0.708 | 6.166 |
| F(000) | 2576 | 3180.0 |
| Crystal size/mm³ | 0.719 x 0.102 x 0.077 | 0.808 × 0.076 × 0.063 |
| 2θ range for data collection | 3.57 to 64.99 | 7.152 to 133.198 |
| Index ranges | -12 ≤ h ≤ 9, -16 ≤ k ≤ 51, -47 ≤ l ≤ 51 | -19 ≤ h ≤ 19, -22 ≤ k ≤ 22, -29 ≤ l ≤ 29 |
| Reflections collected | 32305 | 72951 |
| Independent reflections | 11416 [R _{int} = 0.0506, R _{sigma} = 0.0520] | 25860 [R _{int} = 0.0393, R _{sigma} = 0.0375] |
| Data/restraints/parameters | 11416/120/791 | 25860/1709/1576 |
| Goodness-of-fit on F² | 1.035 | 1.023 |
| Final R indexes [I ≥ 2σ (I)] | R ₁ = 0.0970, wR ₂ = 0.2652 | R ₁ = 0.0522, wR ₂ = 0.1384 |
| Final R indexes [all data] | R ₁ = 0.1265, wR ₂ = 0.2993 | R ₁ = 0.0620, wR ₂ = 0.1485 |
| Largest diff. peak/hole / e Å⁻³ | 1.30/-0.54 | 2.06/-1.76 |

5. Electrochemical studies

5.1 Electrochemical measurements

Electrochemical studies were carried out by using an Autolab Potentiostat, Model PGSTAT101 controlled with NOVA 2.1.4 software. In all experiments, $[N(nBu)_4][PF_6]$ (0.25 M in dry and deoxygenated CH_2Cl_2) was used as the supporting electrolyte with an analyte concentration of 1 mM. Cyclic voltammetry was performed in a cell, under N_2 atmosphere and with disk glassy carbon working electrode, platinum counter electrode, and a silver wire pseudoreference electrode. Measurements were performed at 100 mV s^{-1} scan rate. All scans were referenced to the ferrocenium/ferrocene (Fc^+/Fc) couple at 0 V. Ohmic drop was minimized by minimizing the distance between the working and reference electrodes. The residual ohmic drop was estimated by positive feedback and compensated at 95 %.

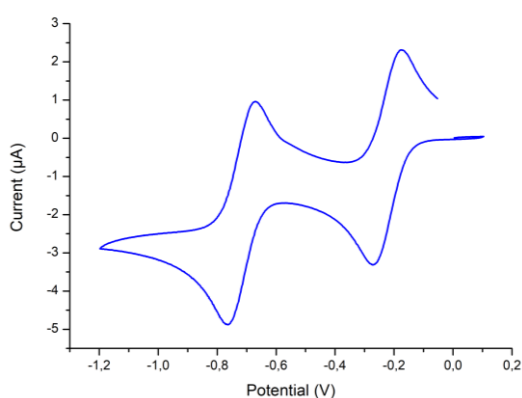


Figure S26. Cyclic voltammogram of **[1a]**(BF₄)₂

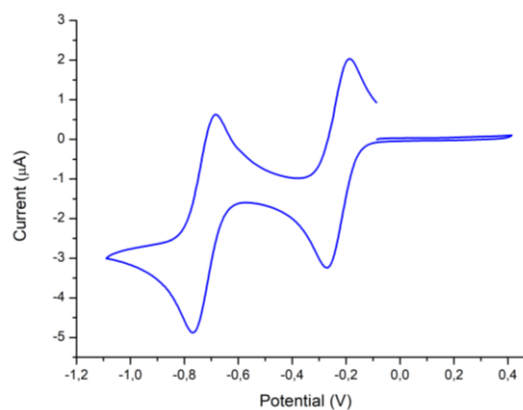


Figure S27. Cyclic voltammogram of **[1b]**(BF₄)₂

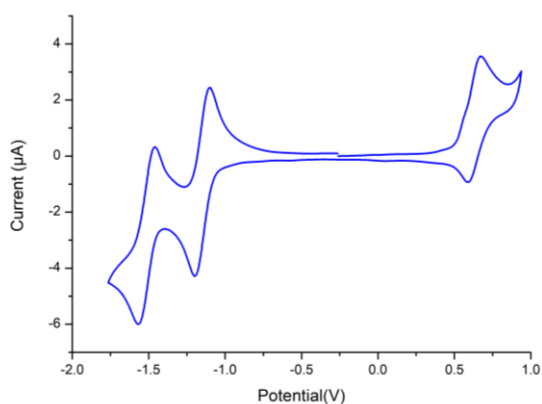


Figure 28. Cyclic voltammogram of **2a**

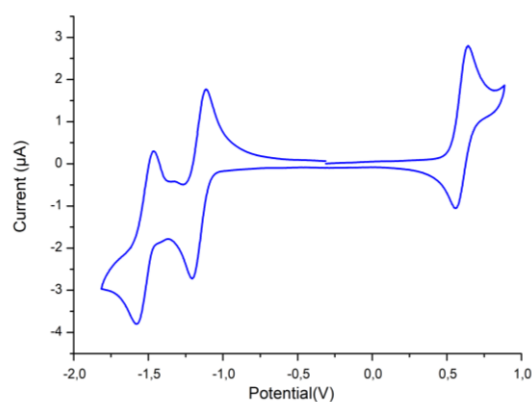


Figure 29. Cyclic voltammogram of **2b**

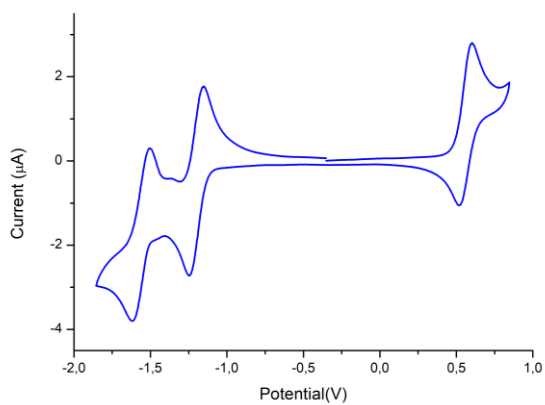


Figure S30. Cyclic voltammogram of 3a

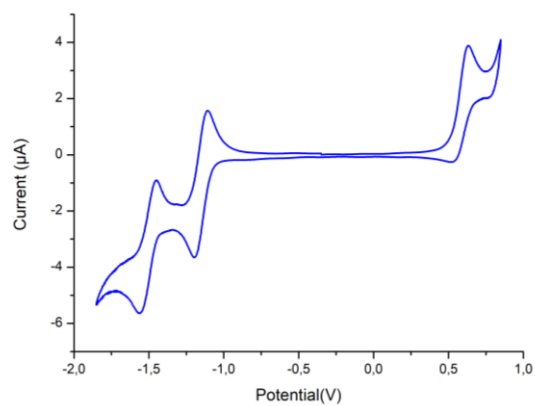


Figure S31. Cyclic voltammogram of 3b

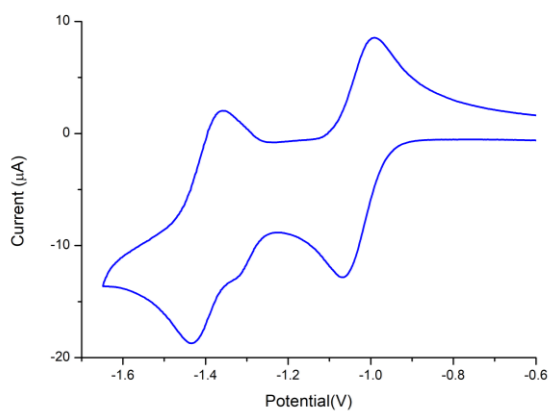


Figure S32. Cyclic voltammogram of 4a

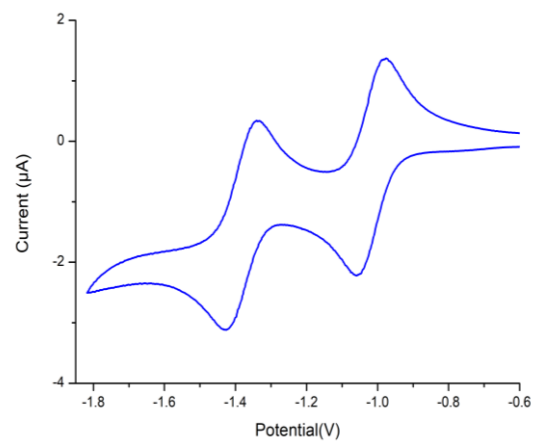


Figure S33. Cyclic voltammogram of 4b

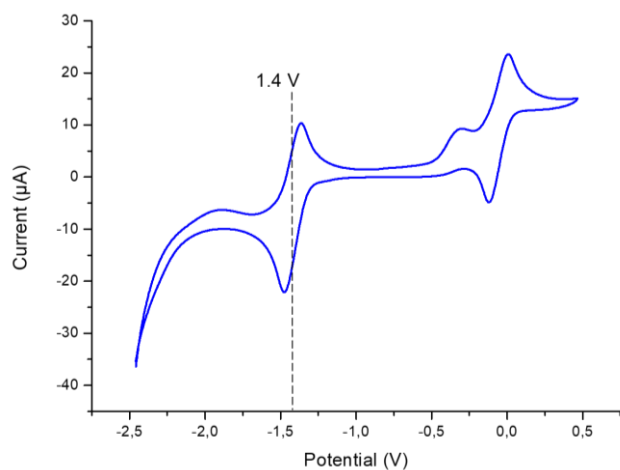


Figure S34. Cyclic voltammogram of cobaltocene

Table S2. Electrochemical properties of compounds **1-4**

| Compound | $E_{1/2}$ (V)/ ΔE (mV) | $E'_{1/2}$ (V)/ ΔE (mV) | $E''_{1/2}$ (V) |
|--|--------------------------------|---------------------------------|---------------------|
| [1a](BF ₄) ₂ | -0.70/69 | -0.23/69 | - |
| [1b](BF ₄) ₂ | -0.71/65 | -0.24/63 | - |
| 2a | -1.51/73 | -1.14/105 | 0.59 |
| 2b | -1.49/71 | -1.16/69 | 0.56 |
| 3a | -1.50/69 | -1.16/71 | 0.57 |
| 3b | -1.49/71 | -1.15/69 | 0.63 ^[a] |
| 4a | -1.39/69 | -1.03/69 | - |
| 4b | -1.39/60 | -1.03/69 | - |

^[a]The Ir(I)/Ir(II) oxidation event is irreversible in **3b**, the value indicated in the table corresponds to the anodic peak potential (E_{pa}).

5.2 Spectroelectrochemical measurements

Spectroelectrochemical (SEC) measurements were performed using a gastight, optically transparent thin-layer solution cell fabricated by Prof. Hartl at the University of Reading (Reading, U.K.), as described previously.^[8] The SEC cell contained a masked Au-minigrid working electrode (32 wires/cm), a Pt-gauze auxiliary electrode, and an Ag-wire pseudo-reference electrode and had CaF₂ windows. In each experiment, electrochemical reduction of the species of interest ([Analyte] = 3 mM for IR experiments and 0.25 mM for UV-vis experiments, [TBAPF₆] = 100 mM in MeCN or CH₂Cl₂ under inert atmosphere) was monitored by the appropriate spectroscopy for a period of 2–5 min. First, the potential of the cell was swept negatively starting at the open circuit potential, recording a thin-layer cyclic voltammogram (5 mV/s) to identify the potential window of interest. Then, fresh analyte solution was introduced in the cell and the potential was varied within range of interest in 33 mV steps. The electrolysis step did not exceed 30 s. After each step an IR or UV-vis spectrum was collected. Diffusion and mixing of the redox products generated at the working and auxiliary electrodes in the cell were reasonably suppressed within the total experimental time (no more than 5 min for one complete measurement).

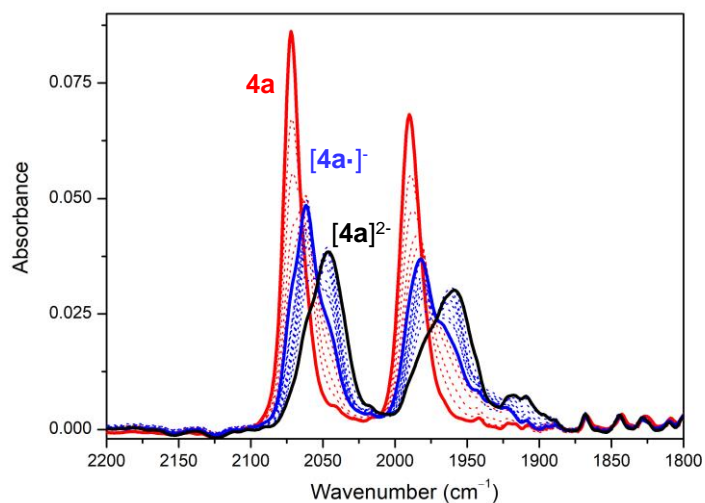


Figure S35 IR-SEC reduction of **4a** in CH_2Cl_2 (0.1 M $[\text{N}(\text{nBu})_4][\text{PF}_6]$). The solid lines represent the IR spectra of **4a** (red), $[\mathbf{4a}]^-$ (blue) and $[\mathbf{4a}]^{2-}$ (black) species.

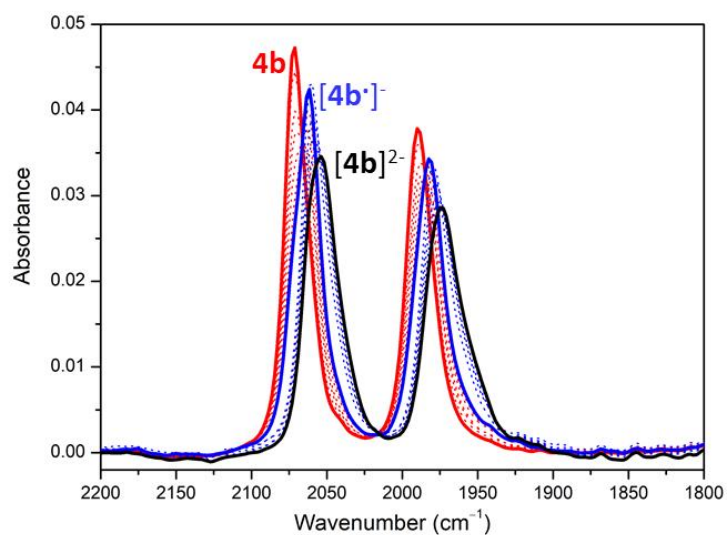


Figure S36 IR-SEC reduction of **4b** in CH_2Cl_2 (0.1 M $[\text{N}(\text{nBu})_4][\text{PF}_6]$). The solid lines represent the IR spectra of **4b** (red), $[\mathbf{4b}]^-$ (blue) and $[\mathbf{4b}]^{2-}$ (black) species.

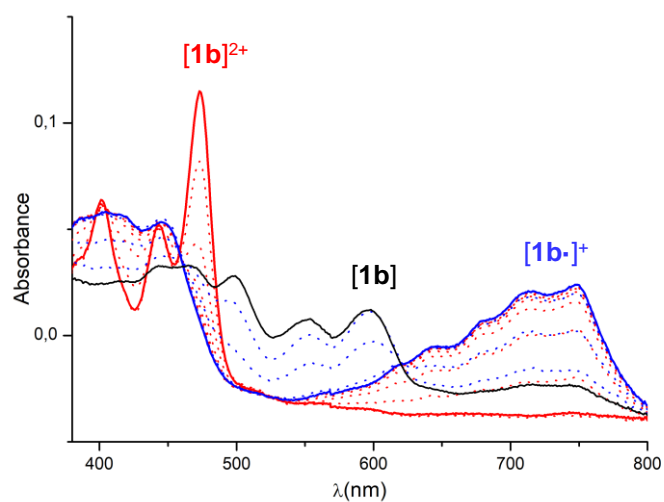


Figure S37. UV-vis SEC monitoring reduction of $[1b]^{2+}$ in CH_2Cl_2 (0.1 M $[N(nBu)_4][PF_6]$). The solid lines represent the spectra of the starting (red), singly-reduced (blue) and doubly-reduced (black) species.

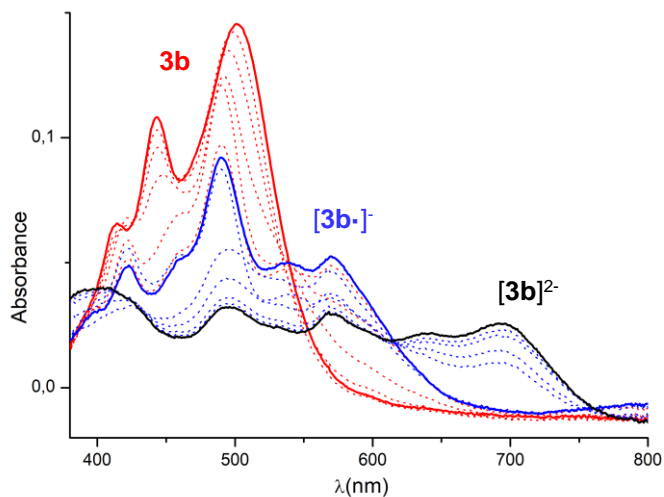


Figure S38. UV-vis SEC monitoring reduction of $3b$ in CH_3CN (0.1 M $[N(nBu)_4][PF_6]$). The solid lines represent the spectra of the starting (red), singly-reduced (blue) and doubly-reduced (black) species.

6. Photophysical properties

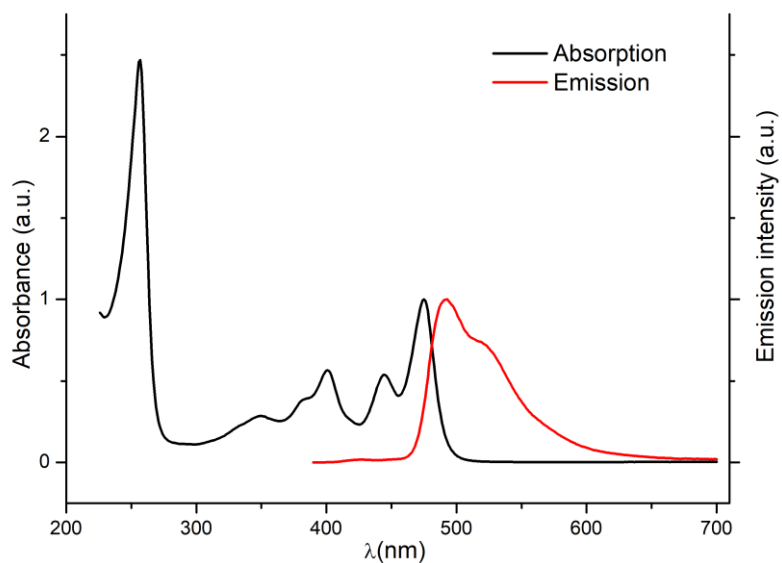


Figure S39. UV-Vis and emission spectra excited at 375 nm of **[1a](BF₄)₂**, recorded in CH₂Cl₂ at a concentration of 50 μ M. Molar extinction coefficients (ϵ , in M⁻¹ cm⁻¹) were determined from Beer's law plots: $\log(\epsilon)$ at 475 nm = 4.33.

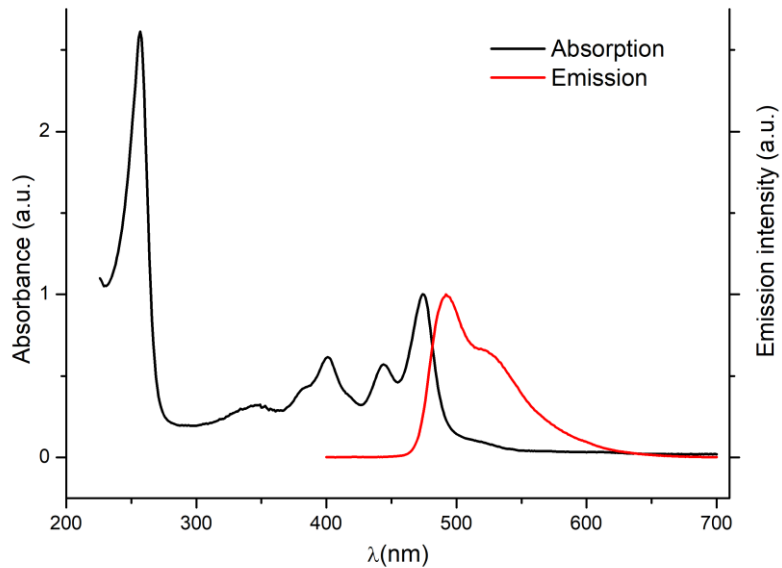


Figure S40. UV-Vis and emission spectra excited at 375 nm of **[1b](BF₄)₂**, recorded in CH₂Cl₂ at a concentration of 50 μ M. Molar extinction coefficients (ϵ , in M⁻¹ cm⁻¹) were determined from Beer's law plots: $\log(\epsilon)$ at 474 nm = 4.00.

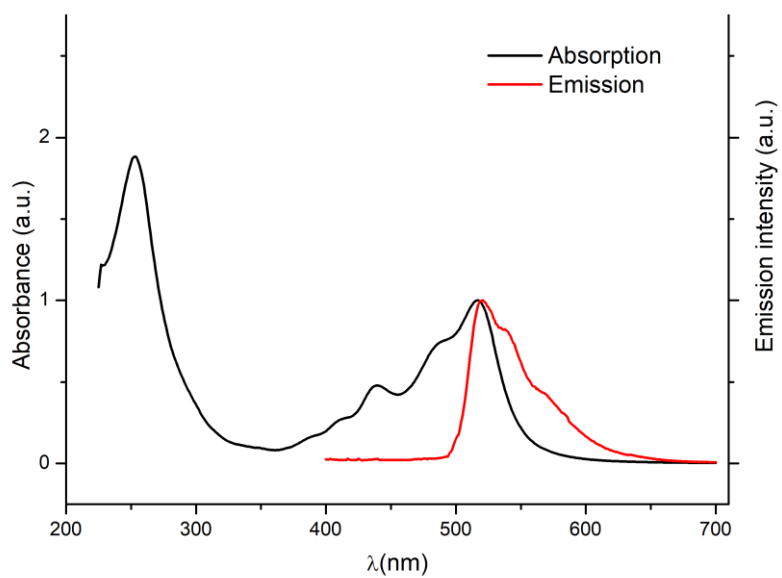


Figure S41. UV-Vis and emission spectra excited at 375 nm of **2a**, recorded in CH_2Cl_2 at a concentration of 50 μM

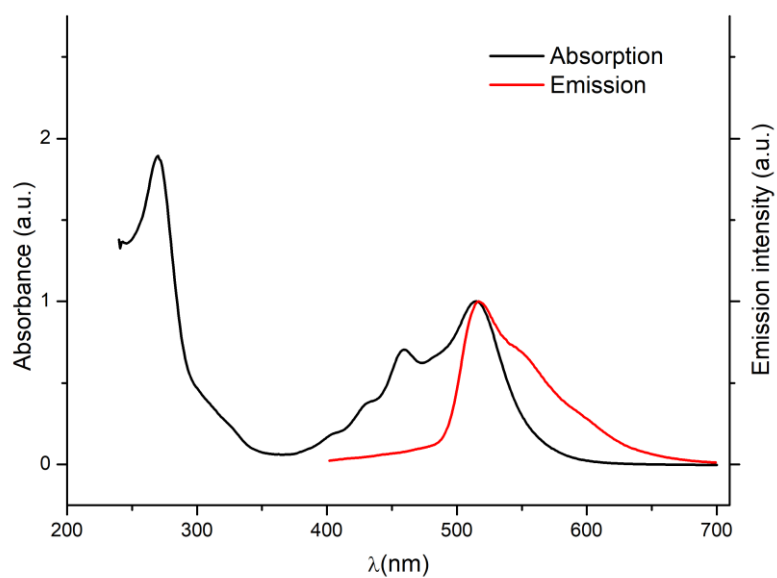


Figure S42. UV-Vis and emission spectra excited at 375 nm of **2b**, recorded in CH_2Cl_2 at a concentration of 50 μM

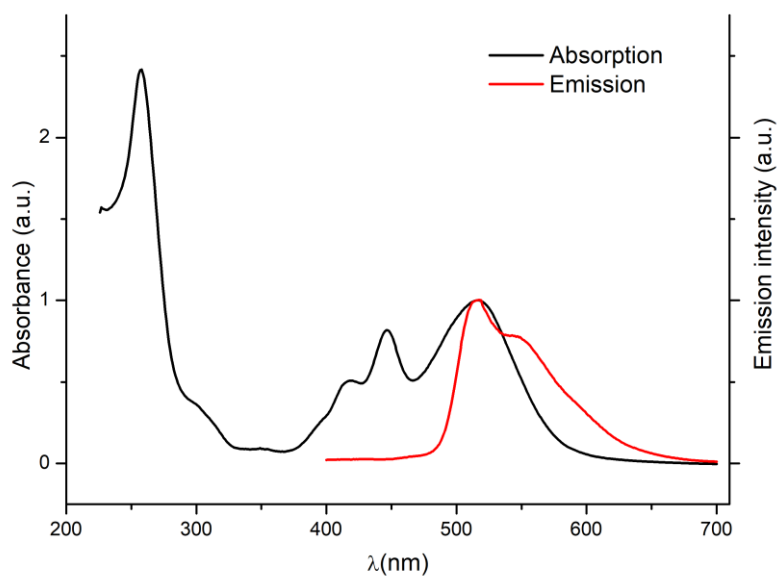


Figure S43. UV-Vis and emission spectra excited at 375 nm of **3a**, recorded in CH_2Cl_2 at a concentration of $50 \mu\text{M}$

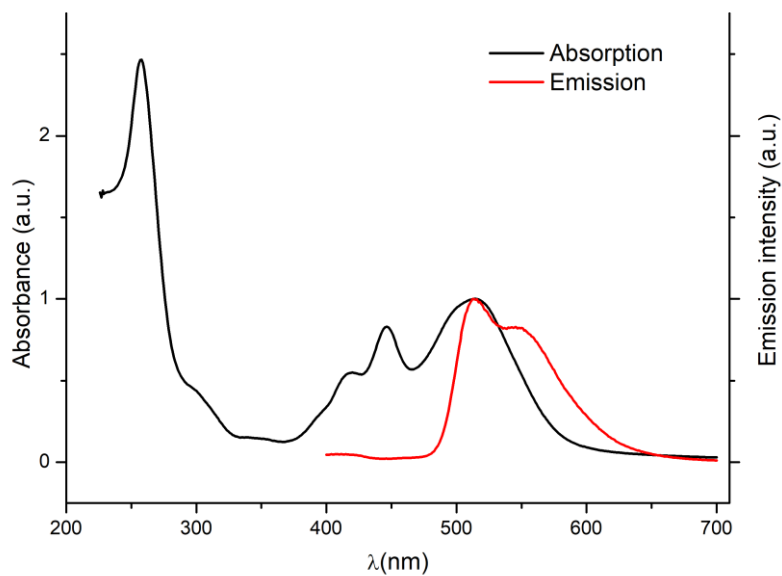


Figure S44. UV-Vis and emission spectra excited at 375 nm of **3b**, recorded in CH_2Cl_2 at a concentration of $50 \mu\text{M}$

Table S3. Photophysical properties of PDI-derived compounds

| Compound | λ_{abs} [nm]^[a] | $\lambda_{\text{em, max}}$ [nm]^[a] | ϕ_{r}^[b] |
|--|---|---|---|
| [1a](BF ₄) ₂ | 475, 445, 401 | 493 | 0.15 |
| [1b](BF ₄) ₂ | 474, 444, 401 | 492 | 0.11 |
| 2a | 517, 488, 439 | 521 | 0.016 |
| 2b | 515, 459, 438 | 517 | 0.015 |
| 3a | 516, 447, 419 | 518 | 0.012 |
| 3b | 514, 446, 420 | 512 | 0.010 |

^[a]Measurements were performed in dry and degassed dichloromethane under ambient conditions. ^[b]Emission quantum yields were measured using a Hamamatsu integration sphere irradiating at 375 nm.

7. Catalytic studies: cyclization of acetylenic carboxylic acids

All the catalytic experiments and manipulations were conducted under Ar atmosphere unless otherwise indicated. Complex $[\text{Fe}(\eta^5\text{-C}_5\text{H}_4\text{COMe})\text{Cp}][\text{BF}_4]^{[9]}$ was prepared according to the literature procedure. All other reagents were purchased from commercial sources.

Cyclization of 4-pentynoic acid to γ -methylene- γ -butyrolactone. In a high pressure Schlenk tube fitted with a Teflon cap, the corresponding catalyst (0.25 mol % or 0.01 mol %) was added to a 0.33 M solution of 4-pentynoic acid (0.5 mmol) and 1,3,5-trimethoxybenzene (0.5 mmol) in CD_3CN . The mixture was heated at 80 °C for 7 h. After this time, the peaks corresponding to the starting material and the product were integrated relative to the internal standard (1,3,5-trimethoxybenzene) by ^1H NMR and GC analyses. γ -Methylene- γ -butyrolactone was isolated as the only product. ^1H NMR (400 MHz, CD_3CN): δ 4.65-4.63 (m, 2H, $\text{C}=\text{CH}_2$), 4.30-4.28 (m, 2H, $\text{C}=\text{CH}_2$), 2.88-2.83 (m, 2H, CH_2), 2.65-2.61 (m, 2H, CH_2). Spectroscopic data were consistent with those reported in the literature.^[10]

Cyclization of 5-hexynoic acid to 6-methylidenetetrahydro-2-pyrone. In a high pressure Schlenk tube fitted with a Teflon cap, the corresponding catalyst (1 mol % or 0.1 mol %) was added to a 0.083 M solution of 5-hexynoic acid (0.125 mmol) in CD_3CN and 1,3,5-trimethoxybenzene (0.125 mmol). The mixture was heated at 80 °C. The peaks corresponding to the starting material and the product were integrated relative to the internal standard (1,3,5-trimethoxybenzene) by ^1H NMR and GC analyses. 6-Methylidenetetrahydro-2-pyrone, was obtained as the only product. ^1H -NMR (400 MHz, CD_3CN): δ 4.56-4.57 (m, 1H, $\text{C}=\text{CH}_2$), 4.32-4.30 (m, 1H, $\text{C}=\text{CH}_2$), 2.60 (t, 2H, $^2J_{\text{H-H}} = 6.8$ Hz, CH_2), 2.52-2.48 (m, 2H, CH_2), 1.87-1.80 (m, 2H, CH_2). Spectroscopic data were consistent with those reported in the literature.^[10b, 11]

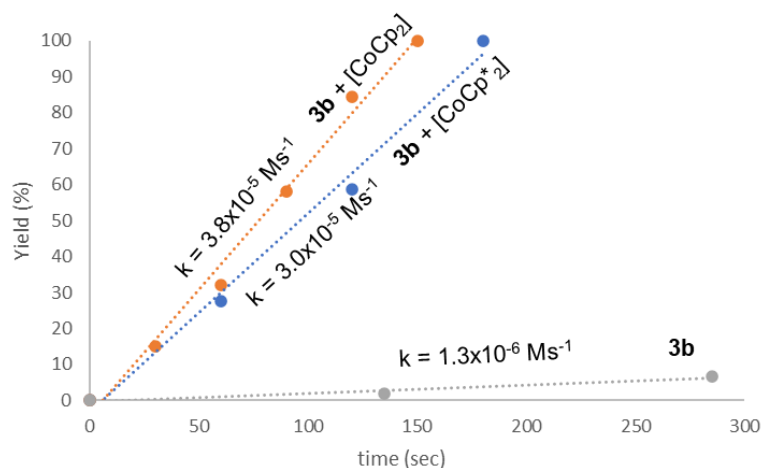


Figure S45. Time-dependent reaction profiles for the cyclization of 4-pentynoic acid using catalyst **3b** with and without addition of cobaltocene or decamethylcobaltocene. The reactions were carried out in acetonitrile, with an initial concentration of 4-pentynoic acid of 0.33 M, and a catalyst loading of 0.25 mol %. Cobaltocene or decamethylcobaltocene were added in a 0.25 or 0.5 mol % with respect to the substrate, respectively. Yields were determined by GC, using 1,3,5-trimethoxybenzene as integration standard. Final yields were also corroborated by ¹H NMR spectroscopy. The figure also shows the kinetic constants for each reaction.

Cyclization of 4-pentynoic acid: redox switching experiments using 3a. A high pressure Schlenk tube fitted with a Teflon cap, was charged with 4-pentynoic acid (103.3 mg, 1 mmol, [acid]₀ = 0.33 M) and 1,3,5-trimethoxybenzene (168.19 mg, 1 mmol). The catalyst was added in solution (0.25 mol %, [catalyst]₀ = 8.3x10⁻⁴ M in CD₃CN). The resulting mixture was heated at 80 °C. After monitoring the reaction over the following 3 hours, the reductant cobaltocene was added to the mixture (1 equivalent with respect to **3a**). The addition of cobaltocene enhanced the reaction rate constant. After collecting data for the following 3 hours, one equivalent (with respect to **3a**) of a chemical oxidant, namely [Fe(η⁵-C₅H₄COCH₃)Cp][BF₄], was added to the reaction mixture. The addition of the oxidant produced a deactivation of the catalytic activity. The oxidant and the reductant were sequentially added separated by periods of 3 hours. The evolution of the reaction was monitored by GC. The conversion was determined by GC comparing the areas of the reagents with the internal standard and corroborated by ¹H NMR spectroscopy by comparing the integrals of the protons of the starting material with those observed in the product.

Cyclization of 4-pentynoic acid. Retention of the redox switchable activity using **3b**.

A high pressure Schlenk tube fitted with a Teflon cap, was charged with 4-pentynoic acid (51.6 mg, 0.5 mmol, [acid]₀ = 0.33 M), 1,3,5-trimethoxybenzene (84.1 mg, 0.5 mmol) and cobaltocene (0.25 mol %). The catalyst was added in solution (0.25 mol %, [catalyst]₀ = 8.3x10⁻⁴ M in 1.5 mL of CD₃CN). The resulting mixture was heated at 80 °C. After monitoring the reaction over the following 3 hours and achievement of full conversion, 0.5 extra mols of 4-pentynoic acid was added and the reaction was allowed to proceed until completion. This experiment was repeated for 3 times without significant deactivation of the catalyst. The evolution of the reaction was monitored by GC. The conversion was determined by GC comparing the areas of the reagents with the internal standard, and corroborated by ¹H NMR spectroscopy by comparing the integrals of the protons of the starting material with those observed in the product.

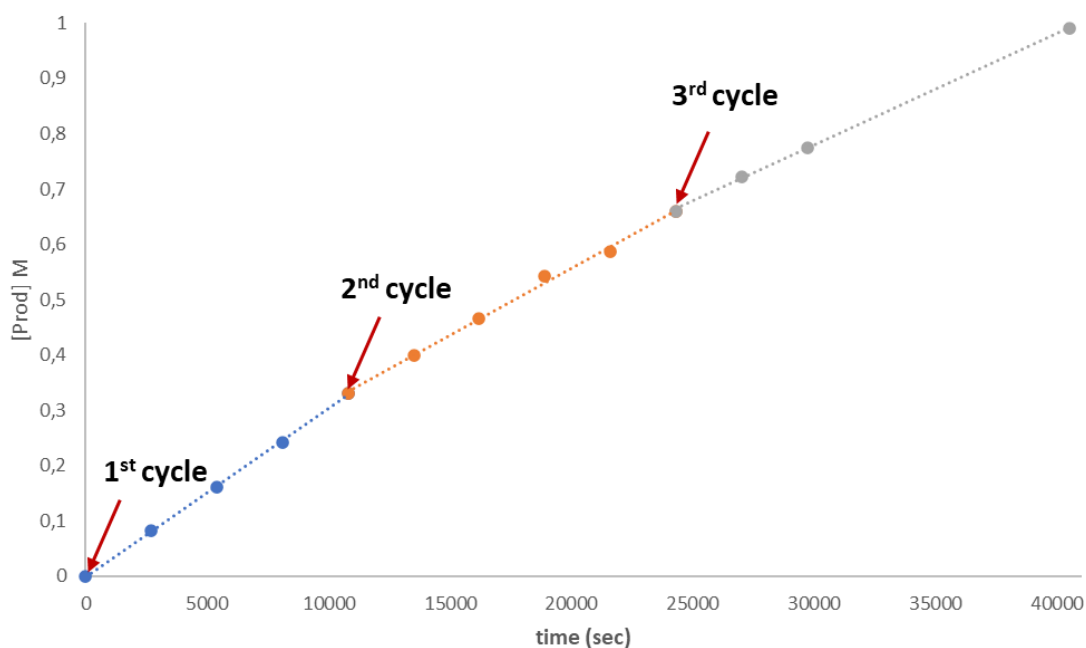


Figure S46. Retention of the activity for the cyclization of 4-pentynoic acid using catalyst **3b** in the presence of cobaltocene. The reaction was carried out in acetonitrile, with an initial concentration of 4-pentynoic acid of 0.33 M, and a catalyst loading of 0.25 mol %. Cobaltocene was added in a 0.25 mol % with respect to the substrate. Yields were determined by GC, using 1,3,5-trimethoxybenzene as integration standard. Final yields were also confirmed by ¹H NMR spectroscopy.

Determination of the reaction order with respect to the catalyst. The reaction order with respect to the catalyst was determined by plotting the concentration of the product against a normalized time scale $t[\text{cat}]^n$ (being n the order of the catalyst), according to the method developed by Dr. Burés.^[12] Visual analysis of the reaction profiles depicted in Figure S47 indicated that the order in the catalyst is 1 (Figure S47c).

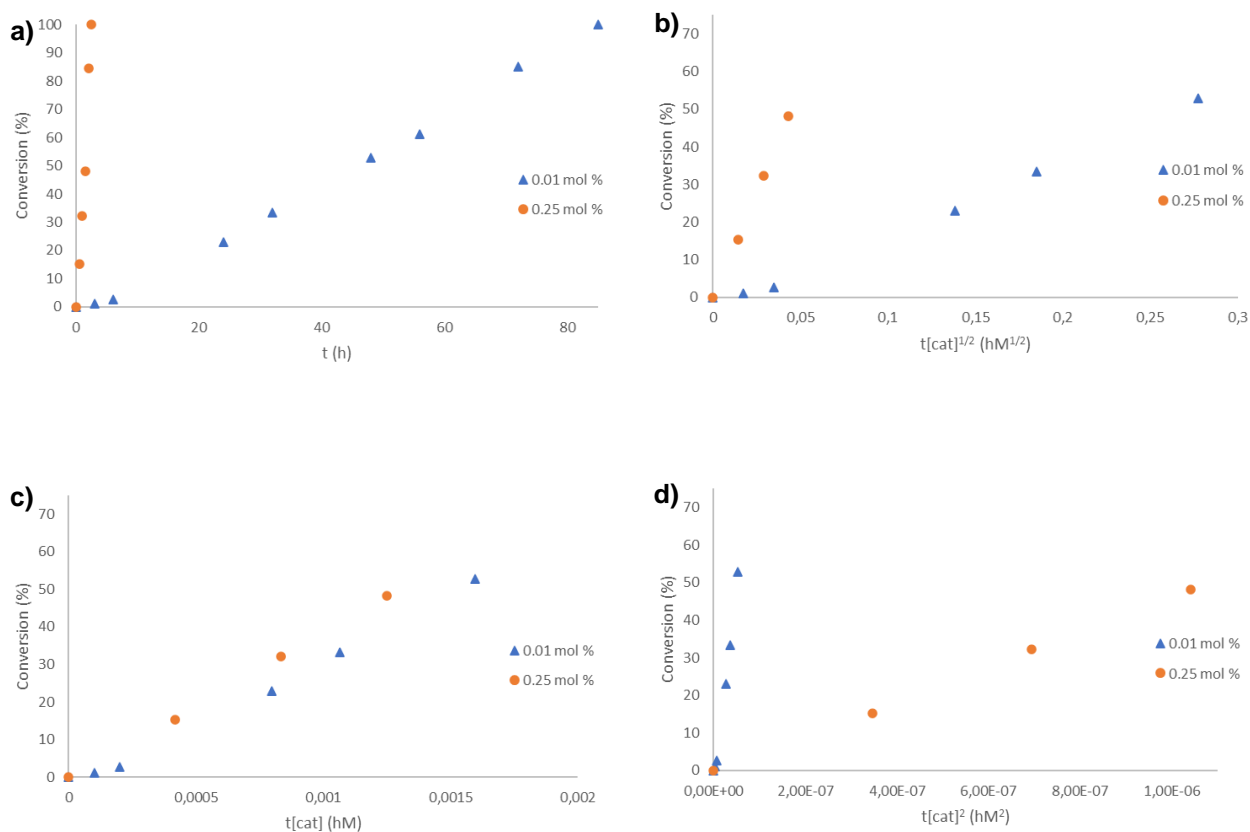


Figure S47. (a) Time-dependent reaction profile of the cyclization reaction of 4-pentynoic acid using catalyst **3b**. (b) Reaction profile with normalized time scale assuming a catalyst order of 1/2. (c) Reaction profile with normalized time scale assuming a catalyst order of 1. (d) Reaction profile with normalized time scale assuming a catalyst order of 2. In all three graphics, the evolution is shown as consumption of 4-pentynoic acid.

8. References

- [1] X. K. Gao, W. F. Qiu, X. D. Yang, Y. Q. Liu, Y. Wang, H. J. Zhang, T. Qi, Y. Liu, K. Lu, C. Y. Du, Z. G. Shuai, G. Yu and D. B. Zhu, *Org. Lett.* **2007**, *9*, 3917-3920.
- [2] a) M. Sasikumar, Y. V. Suseela and T. Govindaraju, *Asian J. Org. Chem.* **2013**, *2*, 779-785; b) S. V. Bhosale, N. V. Ghule, M. Al Kobaisi, M. M. A. Kelson and S. V. Bhosale, *Chem.-Eur. J.* **2014**, *20*, 10775-10781.
- [3] Y. V. Suseela, M. Sasikumar and T. Govindaraju, *Tetrahedron Lett.* **2013**, *54*, 6314-6318.
- [4] G. R. Fulmer, A. J. M. Miller, N. H. Sherden, H. E. Gottlieb, A. Nudelman, B. M. Stoltz, J. E. Bercaw and K. I. Goldberg, *Organometallics* **2010**, *29*, 2176-2179.
- [5] O. V. Dolomanov, L. J. Bourhis, R. J. Gildea, J. A. K. Howard and H. Puschmann, *J. Appl. Crystallogr.* **2009**, *42*, 339-341.
- [6] a) L. Palatinus and G. Chapuis, *J. Appl. Crystallogr.* **2007**, *40*, 786-790; b) L. Palatinus, W. Steurer and G. Chapuis, *J. Appl. Crystallogr.* **2007**, *40*, 456-462.
- [7] G. M. Sheldrick, *Acta Crystallogr. A* **2015**, *71*, 3-8.
- [8] H. L. Wang, L. C. Chen and Y. Xiao, *J. Mater. Chem. C* **2017**, *5*, 8875-8882.
- [9] N. G. Connelly and W. E. Geiger, *Chem. Rev.* **1996**, *96*, 877-910.
- [10] a) R. A. Amos and J. A. Katzenellenbogen, *J. Org. Chem.* **1978**, *43*, 560-564; b) S. Elgafi, L. D. Field and B. A. Messerle, *J. Organomet. Chem.* **2000**, *607*, 97-104.
- [11] G. A. Krafft and J. A. Katzenellenbogen, *J. Am. Chem. Soc.* **1981**, *103*, 5459-5466.
- [12] a) J. Bures, *Angew. Chem., Int. Ed.* **2016**, *55*, 2028-2031; b) J. Bures, *Angew. Chem., Int. Ed.* **2016**, *55*, 16084-16087.